CIRCULATION COPY
SUBJECT TO RECALL
IN TWO WEEKS

UCRL-53496

Heater Test 1, Climax Stock Granite, Nevada

D. N. Montan and W. E. Bradkin

October 1984

Lawrence Livermore National Laboratory

DISCLAIMER

This document was prepared as an account of work sponsored by an agency of the United States Government. Neither the United States Government nor the University of California nor any of their employees, makes any warranty, express or implied, or assumes any legal liability or responsibility for the accuracy, completeness, or usefulness of any information, apparatus, product, or process disclosed, or represents that its use would not infringe privately owned rights. Reference herein to any specific commercial products, process, or service by trade name, trademark, manufacturer, or otherwise, does not necessarily constitute or imply its endorsement, recommendation, or favoring by the United States Government or the University of California. The views and opinions of authors expressed herein do not necessarily state or reflect those of the United States Government or the University of California, and shall not be used for advertising or product endorsement purposes.

Work performed under the auspices of the U.S. Department of Energy by Lawrence Livermore National Laboratory under Contract W-7405-Eng-48.

UCRL-53496
Distribution Category UC-70

Heater Test 1, Climax Stock Granite, Nevada

D. N. Montan and W. E. Bradkin

Manuscript Date: October 1984

LAWRENCE LIVERMORE NATIONAL LABORATORY
University of California • Livermore, California • 94550

Available from: National Technical Information Service • U.S. Department of Commerce
5285 Port Royal Road • Springfield, VA 22161 • $10.00 per copy • (Microfiche $4.50)

Contents

Abstract 1
Introduction 1
Test Description 2
Geologic Setting 2
Experiment Layout 2
Equipment 4
Heaters 4
Thermocouples 6
Packers 8
Pneumatic Control System 8
Pressure Transducers 8
Data-Acquisition System 8
Data Reduction 10
Test Sequences 10
Data Analysis 12
Heater Tests 12
Heater Test Results 13
Permeability Data Analysis 13
Permeability Test Results 17
Conclusions 17
Acknowledgments 19
References 19
Appendix A. Heater Test Data and Calculations A-1
Appendix B. Permeability Test Data and Analysis B-1

Heater Test 1, Climax Stock Granite, Nevada

Abstract

We conducted a series of in-situ tests in the Climax Stock, an intrusive granite formation at the Nevada Test Site, to validate the concept of housing a nuclear waste repository in granitic crystalline rock. The thermal properties of the granite were measured with resistance heaters and thermocouple frames that had been emplaced in drilled holes in the floor of a drift 420 m below the surface. Data analysis was performed primarily by comparing the measured and calculated temperature histories, varying conductivity and diffusivity in the calculations until reasonable agreement was achieved. The best-fit value for in-situ conductivity was approximately 3.1 W/m·K, and the deduced value for in-situ diffusivity was approximately 1.2 mm^2/s. Anisotropic effects in the thermal field were less than 10%.

Permeability was determined by sealing off portions of the drilled holes, using inflatable rubber packers and an air-pressurization system. We then compared the resulting decay in pressure with analytic solutions of the pressure loss from a cylindrical source in an infinite isotropic medium, obtaining a permeability of approximately 1 nanodarcy (nD) at about 30°C. As the temperature increased, the permeability decreased to about 0.2 nD at about 50°C and became too small to measure (<0.02 nD) at higher temperatures.

These tests provided new data on the in-situ properties of a granite typical of the Basin and Range province and significantly advanced our understanding of and ability to perform in-situ thermal and permeability measurements. This knowledge will be of considerable value for future spent-fuel tests.

Introduction

Lawrence Livermore National Laboratory (LLNL) has conducted a series of in-situ tests in the Climax Stock, an intrusive granite formation at the Nevada Test Site. These tests are intended to validate the concept of housing a nuclear waste respository in granitic crystalline rock. The heater test series, which is part of this series of validation tests, was designed to obtain basic technical information on the in-situ thermal conductivity, thermal diffusivity, and permeability of a granite typical of those found in the Basin and Range Province.

The first two tests in the heater series, performed during October 1977 to February 1978, were designed to obtain representative values for the thermal conductivity and diffusivity of a granite under in-situ conditions. They were also designed to determine how dependent these properties were on the principal fracture direction. Both tests centered around electrical heater elements that had been emplaced in a hole beneath the floor of the experiment area, a drift 420 m below the ground surface. An array of thermocouples monitored the temperature history at various distances from the emplaced heat sources. Thermal conductivity and diffusivity were determined from the resulting temperature histories and known heat sources.

The third test, performed during April to July 1978, was designed to determine the in-situ

permeability of the medium as a function of temperature. This was done by "packing off" drilled holes in the granite, pressurizing them with air, and monitoring the subsequent pressure decay. This technique and the test hardware were sensitive enough to determine permeabilities as low as 0.02 nD.

Although this report documents the results of tests conducted several years ago, the results are made available for two reasons: First, the thermal properties data were used in the design of the Spent Fuel Test—Climax[1]; hence, their source must be available for reference. Second, the permeability values and the analytical methods used to determine those values are not available elsewhere. They are expected to become increasingly important now that crystalline rocks are again being considered for a permanent nuclear waste repository. For related test information, see Refs. 2 to 5.

Test Description

Geologic Setting

The Climax Stock is a composite granitic intrusive body located near the northeast corner of the Nevada Test Site, about 100 km northwest of Las Vegas. It is named for the Climax tungsten mine, located in Paleozoic rocks north of the granitic outcrop. The Stock, which outcrops over an area of about 4 km^2, has been explored extensively in support of past nuclear test activities. Geophysical evidence suggests that the Stock expands conically to an area of about 100 km^2 at a depth of several kilometers.

The granitic Stock is composed of two main units—granodiorite (to the north) and quartz monzonite (to the south)—that contain varying proportions of the same minerals. Both units have a grain size of about 1 to 4 mm, but the quartz monzonite, which is richer in feldspar, contains scattered large feldspar crystals ranging up to 50 mm in length. The heater tests were conducted in the quartz monzonite unit. The test level (420 m depth) is apparently above the water table, and the granite appears to be unsaturated. However, about 1 to 2 wt% water is localized in fractures and pores and should be free to migrate under thermal or pressure gradients.

The in-situ stress environment near the test area was measured using the overcoring technique. The least principal stress was 2.75 MPa oriented N42°W/ − 14° and the maximum principal stress was 11.56 MPa oriented N56°E/ − 29°.[6] These measurements also indicated that significant variations in stress (as a result of the excavated drifts) extended about 1 m into the rock. The ambient rock temperature at experiment depth was 23°C.

Experiment Layout

The experimental site is near the bottom of a 425-m-deep shaft (2 by 4 m in cross section) that was constructed more than 15 years ago in support of two nuclear weapons effects tests. The first nuclear detonation in the Climax Stock was the 5-kt Hardhat event (February 1962), with the detonation point 286 m below the surface and about 245 m from the shaft. The second was the 61-kt Piledriver event (June 1966), at a depth of 463 m and about 430 m from the shaft.

The heater tests were conducted beneath the floor of an existing drift that was about 3 m wide and a 3-by-4-m alcove that was excavated for the tests. An array of 17 small-diameter holes was drilled into the floor, using diamond core bits and water as a circulating medium. Of these, 13 were AX (48-mm-diam) holes for thermocouple emplacement, two were NX (76-mm-diam) holes for a U.S. Geological Survey (USGS) add-on experiment, and two were NX/AX stepped holes for the heaters. This array, shown in Figs. 1 and 2 and described in Table 1, is in an orthogonal pattern that is oriented approximately parallel and perpendicular to the major fracture system in the immediate vicinity. The two heater holes were near the ends of the array, with the thermocouple holes at horizontal ranges of approximately 0.2 to 5 m from the heaters. The 5-m hole was at the

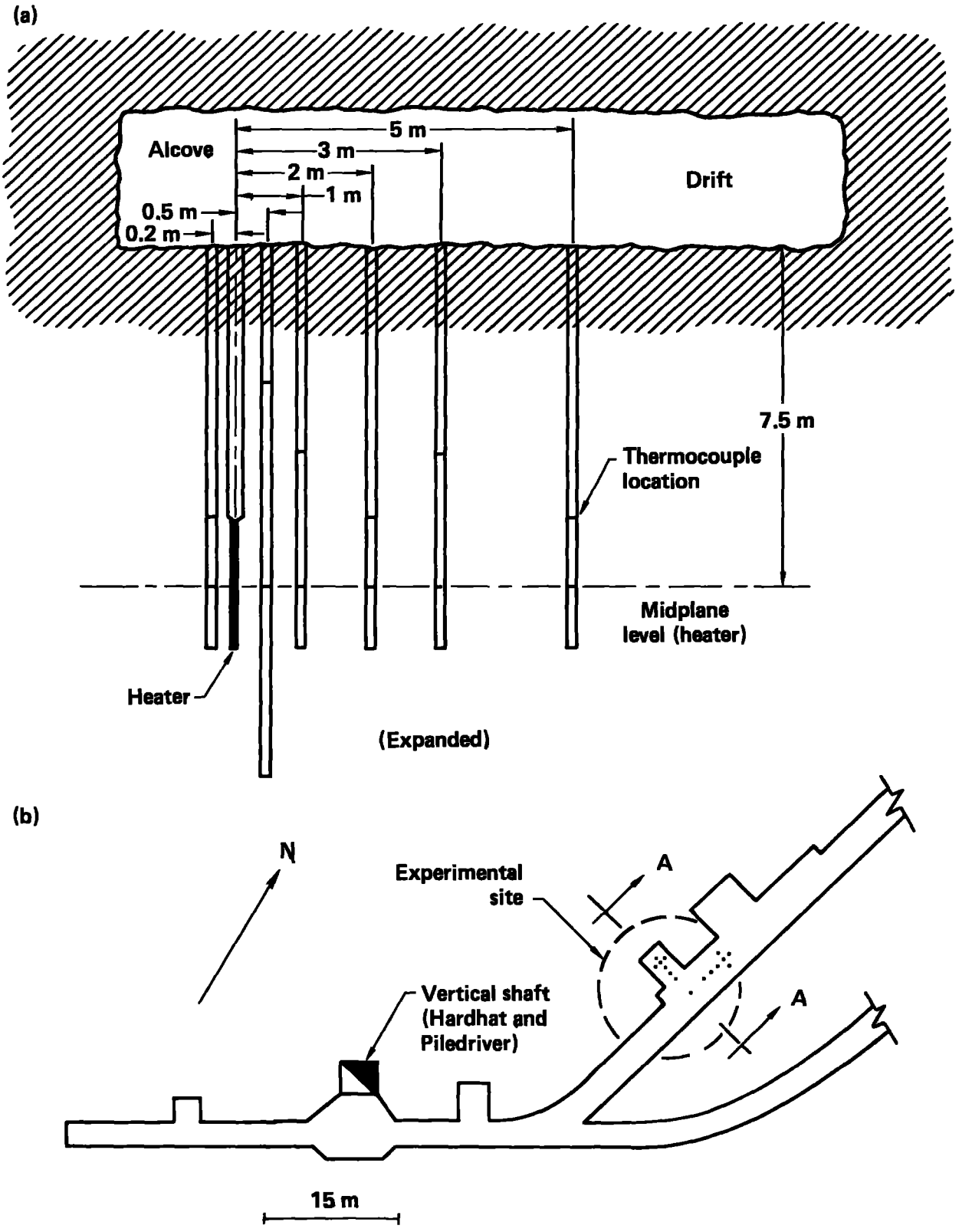

Figure 1. (a) Vertical cross section and (b) plot plan.

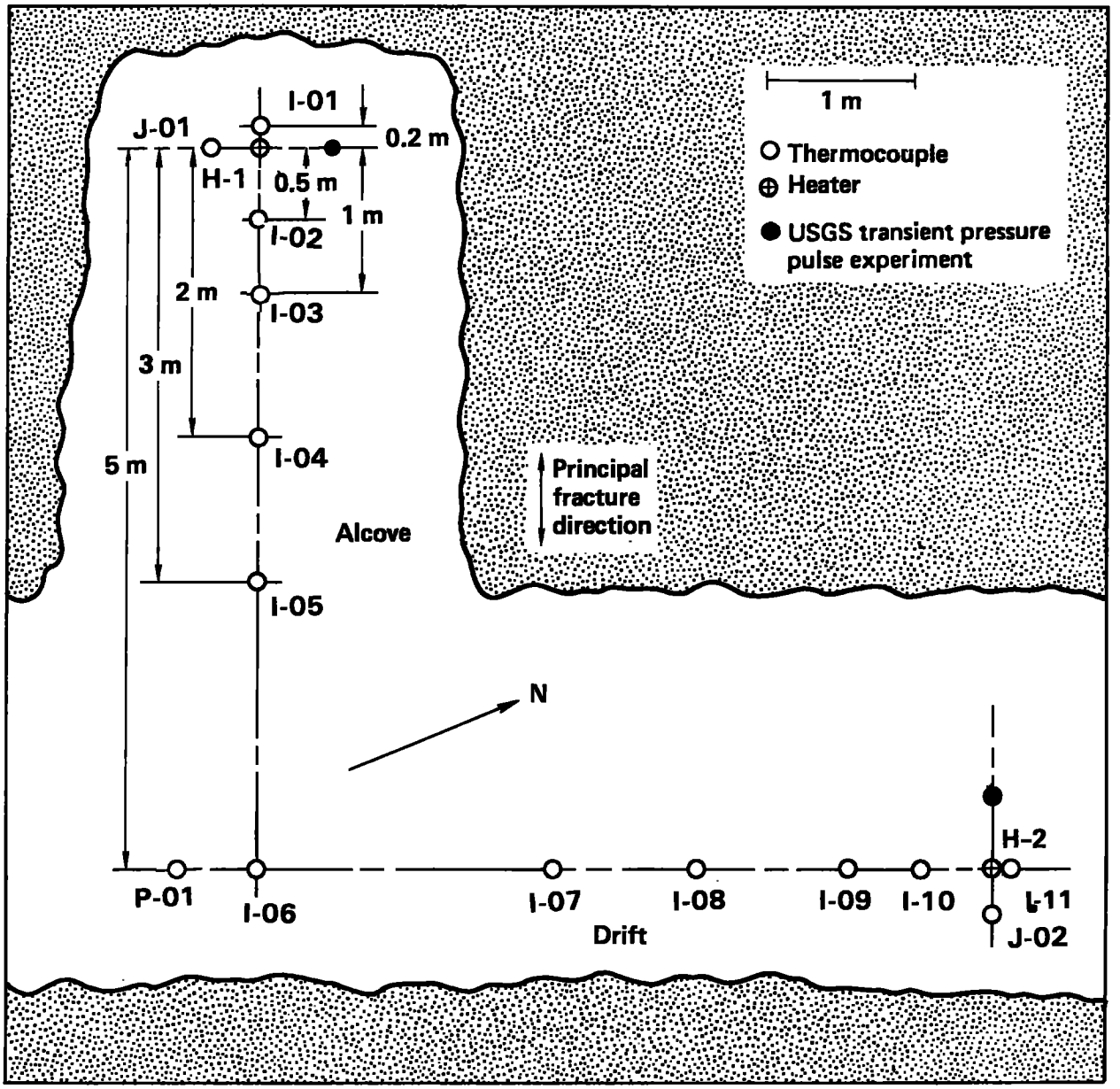

Figure 2. Heater test layout.

intersection of the two orthogonal lines of the array. The holes were all 9 m deep except for two which were 12 m deep. The heater midplane was at a depth of 7.5 m.

All of the holes were surveyed optically with depth, using a movable light-source target. Thus, the as-built location of the thermocouples with respect to the heaters is known.

Equipment

All control and data-acquisition was normally handled in a trailer on the surface because of the expense (about $1000 per day) involved in maintaining personnel access to the underground area and the expected duration of the experiment. Appropriate multiconductor shielded cables were run from the surface to the underground area by means of a 6-in.-diam conduit in the access shaft.

Heaters

The cartridge-type resistance heaters were rated for 5.28 kW at 240 V and had an active heating length of 2.9 m. For the first test (H-1), the active elements were encased in a Inconel sheath that was slightly longer than the 2.9-m active

length. The heater sheath was suspended at the NX/AX step by a 64-mm-diam flange and hung freely with a 38-mm-diam disk at the bottom.

Table 1. Horizontal ranges of test array.

Hole	Nominal range from heater (m)	As-built range from heater at midplane (m)
H-1		
I-01	0.2	0.285
I-02	0.5	0.499
I-03	1.0	1.145
I-04	2.0	2.005
I-05	3.0	2.821
I-06	5.0	5.053
J-01	0.3	0.407
H-2		
I-06	5.0	4.926
I-07	3.0	2.984
I-08	2.0	1.792
I-09	1.0	0.735
I-10	0.5	0.369
I-11	0.2	0.399
J-02	0.3	0.405
P-01	5.3	5.23

Two pins through a ceramic plug at the top of the sheath provided for electrical connections. The second heater was identical except that the sheath was 19 mm in diameter.

Initially, the heaters were emplaced using a tubing string that was then disengaged and removed from the holes. A later modification (developed after a short circuit) brought the power leads from the heater to the drift floor inside a permanent string of aluminum tubing with swaged fittings. The tubing isolated the power leads and connections from the water that refluxed above the heater. A short length of mineral wool insulation was wrapped around the tubing above the heater, and the rest of the hole was backfilled with loose Perlite insulation. Figure 3 shows the heater assembly and the three thermocouples banded to it. The thermocouples, located near the top, bottom, and midpoint of the active part of the heater, were used to verify that the heater was operating and not at an excessive temperature.

The power level to each heater was set by a silicon-controlled rectifier (SCR) controller that

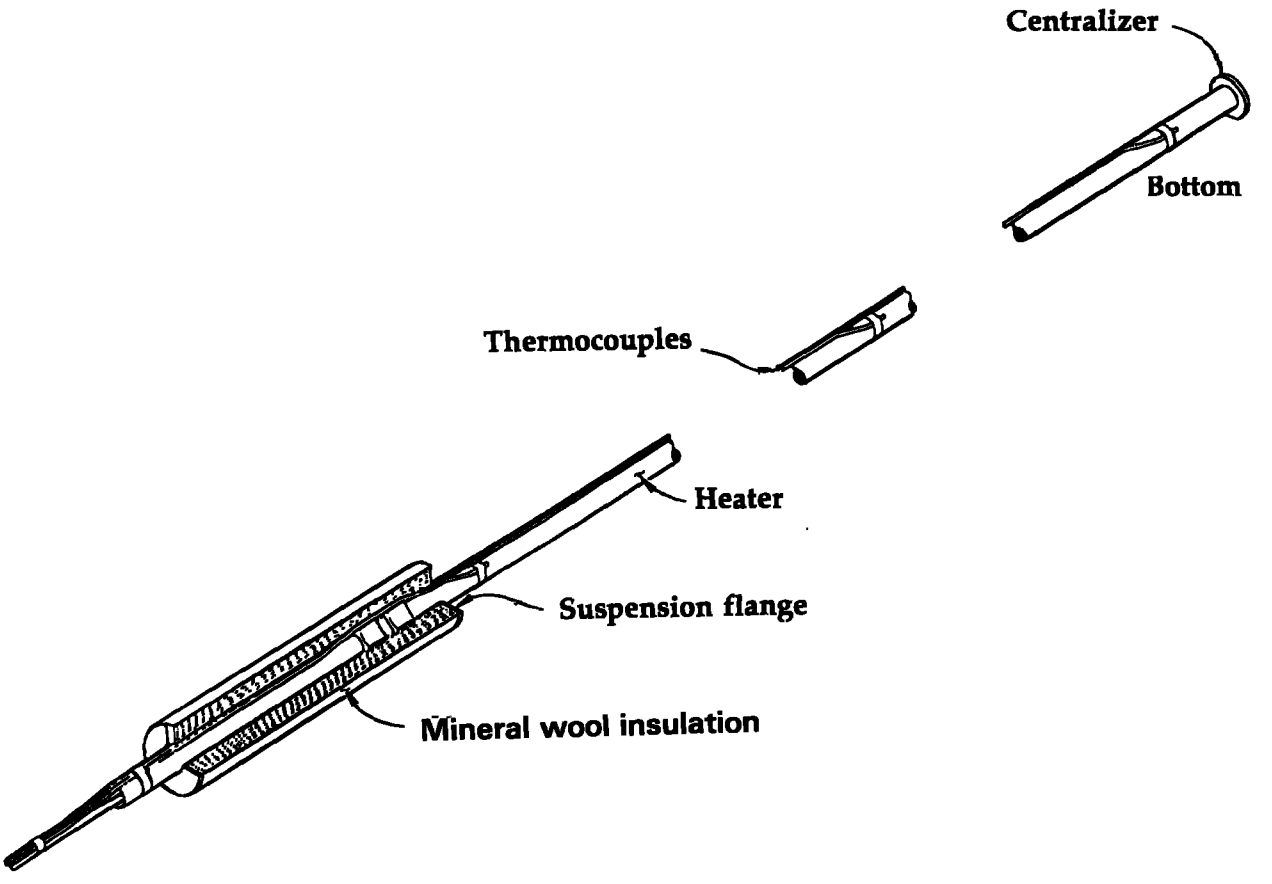

Figure 3. Heater assembly.

provided a 0 to 100% variable duty cycle. The power levels could be set locally at the controllers in the drift and remotely at the surface station. The actual power level of the heaters was monitored with power transducers that provided a direct-current (dc) voltage proportional to the power output of the controller. This voltage, along with the thermocouple voltage, was recorded by the data-acquisition system at the surface.

An identical heater, suspended from a packer on a stainless steel tubing gooseneck, was used for the permeability tests. The bottom centralizing disk was replaced by a spring centralizer, providing for easier emplacement and retrieval (Fig. 4).

Thermocouples

The thermocouples used were Type K (Chromel–Alumel), 28-gauge wire, in 100-ft lengths, with 1/16-in. Inconel 600 metal sheaths and magnesium oxide insulation. The hot junctions were ungrounded. We chose Type K thermocouples because they were suitable for our expected temperature range and because of the relatively high Seebeck coefficient. The sheaths, which were oxidation-resistant, were chosen to minimize or prevent damage to the thermocouple wires and junctions and appear to have been successful.

In addition to the six thermocouples on the heaters (three on each heater), we emplaced four thermocouples in each of the 13 instrumentation holes. The emplacement technique was designed with three objectives in mind: accuracy of location, contact with the rock, and removability (for replacement if necessary and for future use of the holes). A typical 3-m-long thermocouple assembly is shown in Fig. 5. We used similar assemblies for the two holes in which the thermocouple measurements spanned more than 3 m; in both cases, however, the vertical clearance in the drift required that the assemblies be made up of modules of 3 m or less.

The hot junctions of the thermocouples were silver soldered to 6-mm-diam copper pins that protruded through ceramic collars in the frame. The assemblies were then emplaced by a two-step process. First, we lowered the frame into position, with the pins retracted and perpendicular to the direction of the heater. Then, the lowering tube string was disengaged at a J-slot fixture and removed. In the second step, we inserted a "spear" of 13-mm-diam stainless steel tubing down the

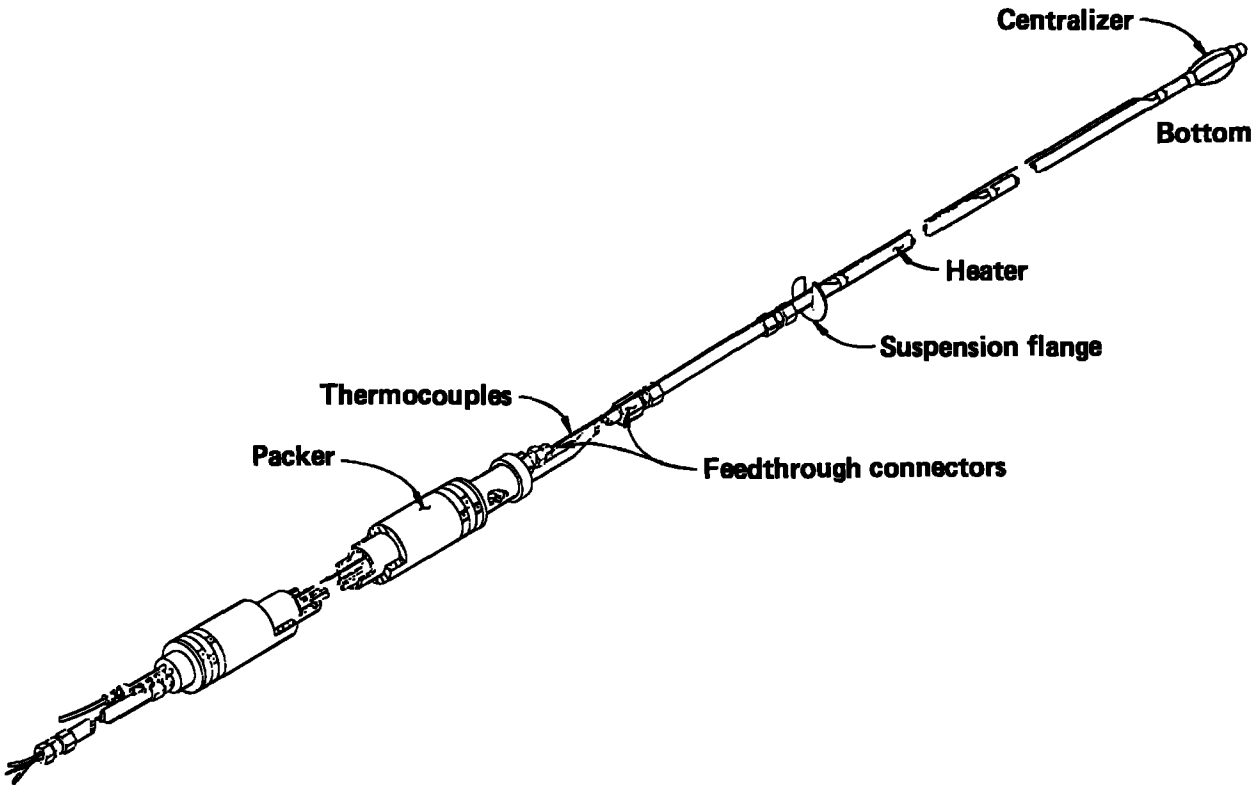

Figure 4. Heater packer assembly.

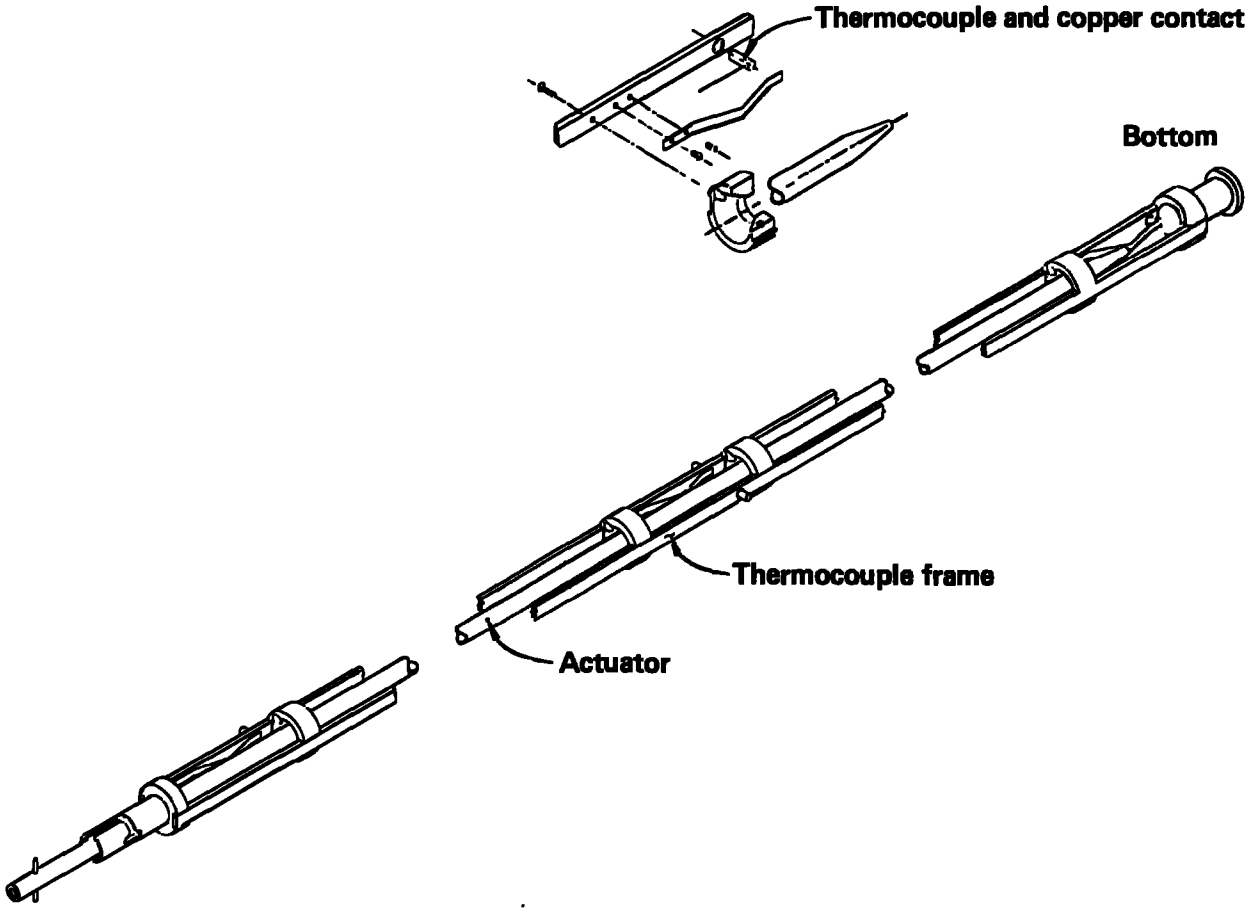

Figure 5. Thermocouple assembly.

central axis of the frame, activating the springs and driving the copper pins firmly against the rock. Again a J-slot fixture was used to disengage the spear. The holes were backfilled with loose Perlite insulation.

For the permeability tests, we used an in-place actuating rod with approximately 25-mm axial travel that allowed the pins to remain retracted during emplacement and to be driven into contact with the surrounding rock when they reached total depth. The entire assembly was suspended below an inflatable packer (see Fig. 6).

A three-wire, 60-channel, ambient reference junction block located in the alcove was used to terminate the thermocouples and to connect them to the shielded copper pairs leading to the surface data-acquisition system. When surrounded with plastic foam insulation, this large metal block with insulated connecting terminals imbedded in it provided a uniform (albeit varying with ambient temperature) "cold" junction.

The block temperature was monitored initially by an attached thermocouple. The output of this thermocouple was processed by a "thermocouple transmitter unit" mounted next to the reference block. This unit purportedly contained an equivalent ice-point reference and circuitry to provide an output suitable to reference all the thermocouples to 0°C. Because the unit proved to be noisy and temperature-sensitive, we used the lower thermocouple in the hole farthest from the heaters as a reference point during the first part of the experiment. Later, we drilled a long (~15-m) hole into the wall of the drift across from the alcove and placed two spare thermocouples in it to provide a constant reference temperature. Two more thermocouples in the experimental area were occasionally placed in an ice bath to provide a reference calibration. Eventually, we replaced the "transmitter unit" with a unit that proved to be at least 10 times as stable, although the earth itself was more stable.

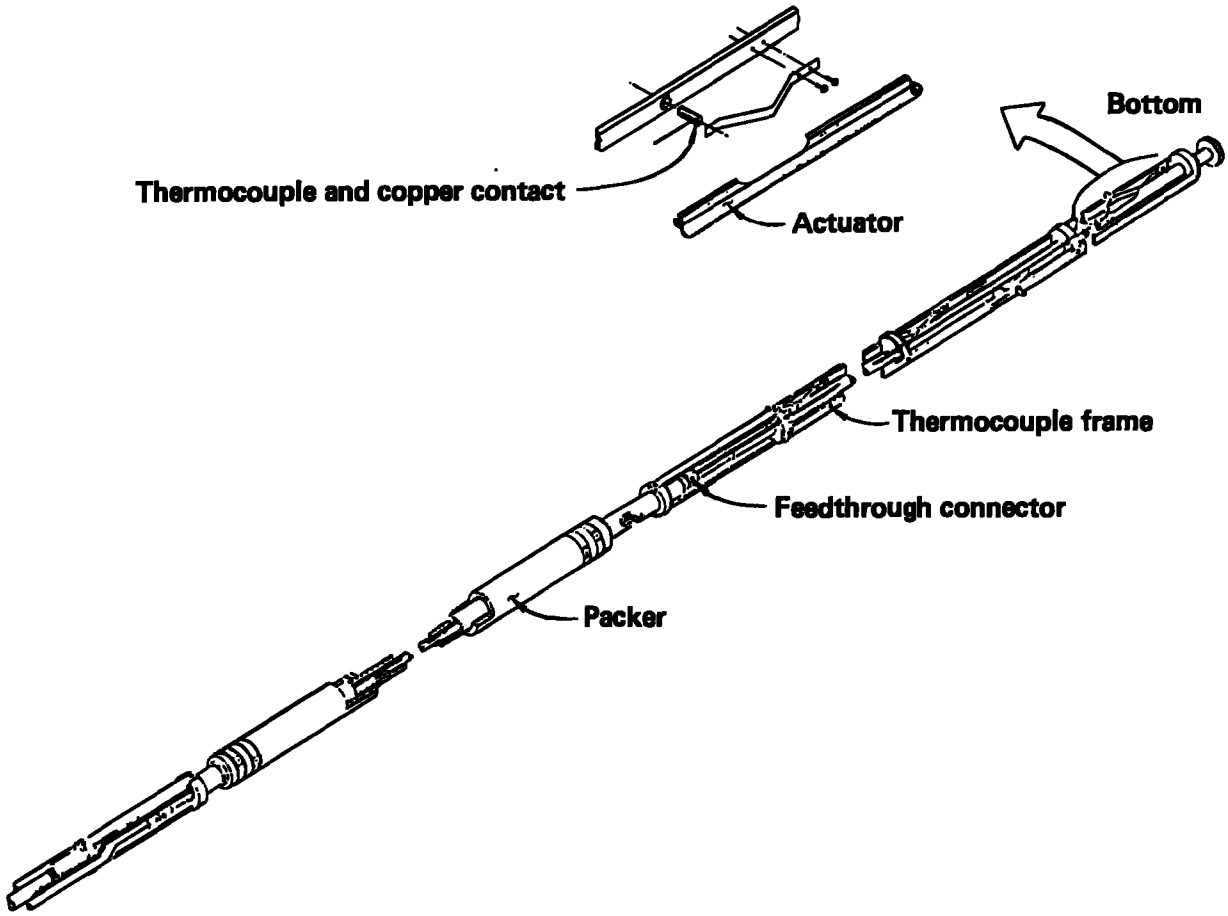

Figure 6. Thermocouple packer assembly.

Packers

Packers were fabricated using rubber sleeves banded to stainless steel pipe mandrels. Stainless steel tubes were welded through drilled holes in the pipe wall to inflate the packer and to control the pressure in the sealed portion of the hole. Thermocouples were also emplaced within the pressurized region of the packed-off holes.

Pneumatic Control System

Air control and monitoring equipment was mounted on a panel in the tunnel. Each of the five holes instrumented for permeability testing was provided with two flexible nylon tubing strings, one for packer inflation and one to control hole pressure. Air was supplied from a rack of compressed air bottles, packers were inflated with manual valves and dial gauges, and hole pressure was controlled by remotely controlled solenoids and pressure transducers. In this way, once the packers were set, experiments could be conducted entirely from the surface, with no need for tunnel access (Fig. 7).

Pressure Transducers

The Teledyne Taber Series 185 and Series 206 transducer units used for the permeability experiment had an operating range of 0 to 300 psia. Each was calibrated at the LLNL standards laboratory and had an output linear to within 0.25% of full-scale. Repeatability was within 0.1% of the full-scale output. Within a compensated temperature range of −30 to +170°F, the thermal zero shift was less than 0.01% and the thermal sensitivity was within 0.005% of full-scale output per degree Fahrenheit.

Data-Acquisition System

The data-acquisition system was basically two 60-channel data logger units located on the surface in an air-conditioned trailer near the shaft. Figure 8 is a schematic of the data and control system. A Fluke Model 220A was the primary

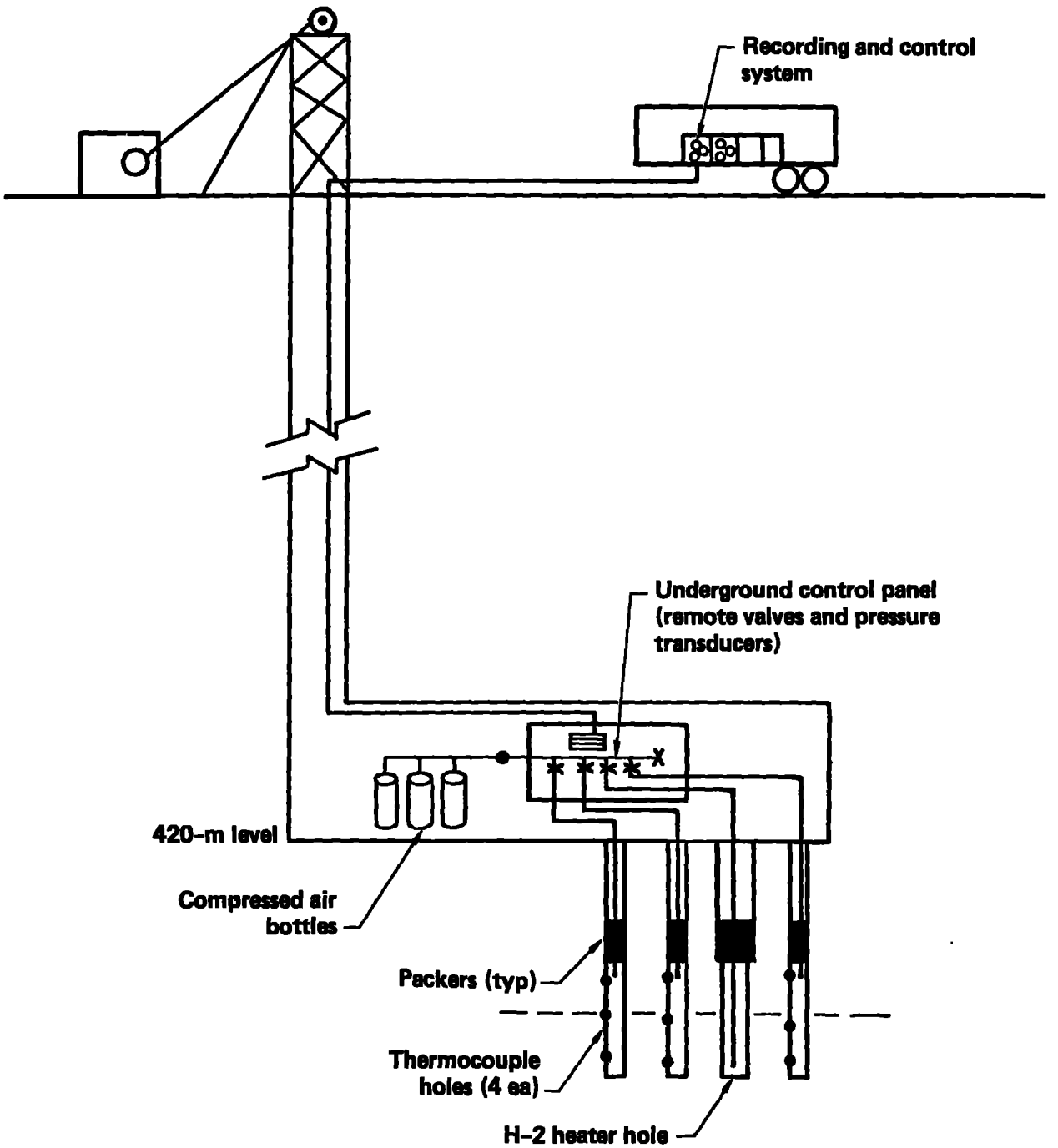

Figure 7. Pneumatic control system.

unit; a Vidar Model 5203D was available as a backup. Although both units provided a hard-copy printout of monitored voltages and a magnetic tape recording of the same data, only one unit at a time could be used to record the data.

The system normally operated unattended, recording data at set intervals (usually one-half or one hour). Every workday, a technician checked the system and called Livermore to report the latest data channel readings of interest. Each week (approximately), the printout and magnetic tape were sent to Livermore for data reduction.

Data Reduction

All data reduction was done at LLNL. No attempt was made to combine signals such as reference voltages at the data-acquisition system or in the experimental area. This decision proved to be wise because it allowed us to choose, post facto, the best temperature reference(s) to use.

Data reduction was basically a three-step process:

1. The tape from the field was copied to a disk file on one of the large computers at LLNL.
2. Errors were corrected where possible, and bad records were removed individually with an interactive text-editing routine.
3. The "cleaned-up" file was read and processed by a computer program written specifically for the experiment. Output consisted of hardcopy listings of raw and converted data and of files that could be merged with previous output to produce time-history data plots.

Test Sequences

The test sequences were not planned in great detail. The basic plan was to operate the first heater at somewhat less than maximum power for a period of two to three weeks and then, depending on the behavior of the system, to change the power level periodically to obtain temperature histories from which both conductivity and diffusivity could be inferred.

The first heater test (H-1) used the heater in the alcove and was operated for a total of 68 days from 14 October to 21 December 1977; its power history is shown in Fig. 9. To ensure that we did not overheat the heater, we brought the power up stepwise during the first few hours. After about nine days, the test began to control the sequence.

A small amount of water, probably circulating fluid lost to the fracture system during drilling, entered the heater hole as vapor and began refluxing in a region near the top of the heater. This

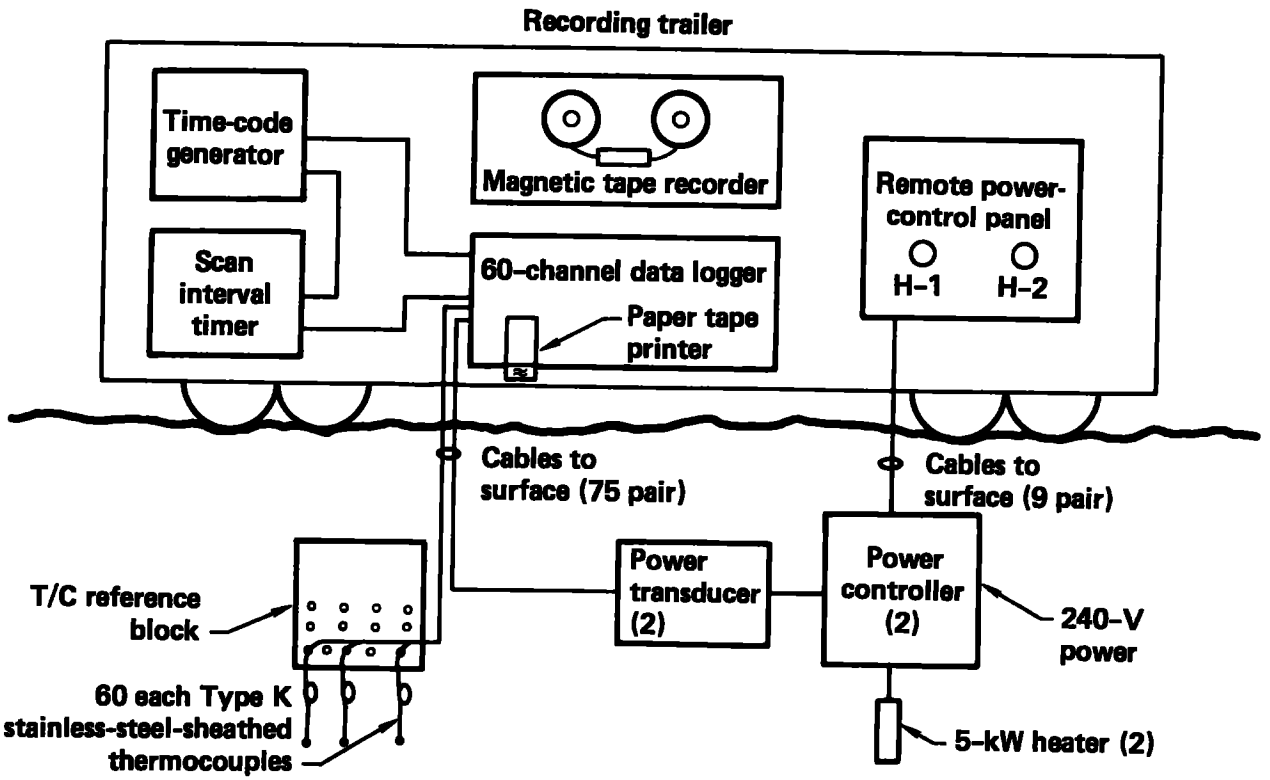

Figure 8. Data and control system for heater test.

refluxing eventually caused a short circuit in the power leads, which, in turn, caused the SCR in the controller to fail open. After repairs were made, the system operated at the set power level for about a week until the controller failed full on and the power level rose to 4.8 kW. This failure was apparently caused by a transient short circuit in a heater lead. Because the heater temperature at 4.8 kW was not excessive and everything else was working well, we let the system run this way for about one month. Then, we turned the heater off for five days to make repairs. When the repairs were completed, we turned the heater back on at the original 3.7-kW level and operated it for another three weeks.

The second heater test (H-2) used the heater in the drift and operated for 62 days from 21 December 1977 to 21 February 1978; its power history is shown in Fig. 10. This test was intended to be similar (but not in detail) to H-1. The only unanticipated power change was termination of the high-power (4.8-kW) phase, when the temperature at the bottom of the heater began to rise. This excursion was subsequently associated with the accumulation of fine granite dust (probably drill cuttings) at the bottom of the heater. Water refluxing above the heater was also indicated; however, it caused no problem because of the improved configuration.

The permeability test ran for 83 days from 13 April to 7 July 1978. It included a total of seven pressurization test cycles, six of which yielded interpretable results. During calibration and checkout, we established, within the resolution of the instrument, that there was no pressurized air communication between any of the holes in the instrument array. Permeability was obtained by air-pressurizing each hole quasi-instantaneously and observing the pressure decay with time. Typically, during a 100-h period, the pressure would decline from 750 kPa to between 700 and 730 kPa. The resolution of the pressure-transducer recording was 0.05 kPa.

Ideally, no temperature change would occur during a permeability test; thus, all changes in pressure would be caused by fluid flow away from the drill hole. Because it would have taken months at each power level to attain a constant rock temperature at the range of the test holes, we reduced the power level before each pressurization test, which produced a nearly constant temperature during the first few days of testing (Fig. 11). With this technique, we were able to control test-hole temperatures to $\pm 1°C$ during the first two tests at elevated temperature.

Before energizing the heater, we ran an initial test and then conducted two additional tests at elevated temperature. To establish a maximum temperature plateau, we then turned up the heater to full power. After 200 h at full power the heater failed internally, and we had to modify the test sequence to evaluate permeability during the cool-down cycle. During this cycle, two valid tests were conducted.

These initial tests were conducted in rock that had been thermally cycled during the previous tests. As a final check on in-situ permeabilities, we moved two of the test assemblies to holes near the intersection of the orthogonal array (I-06 and P-01) so that we might evaluate the permeability of the rock mass in an area where no significant heating had occurred.

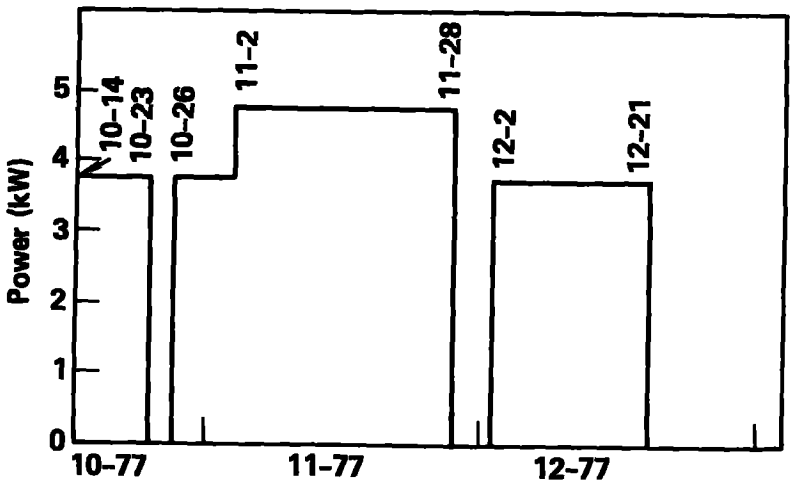

Figure 9. Power history of H-1.

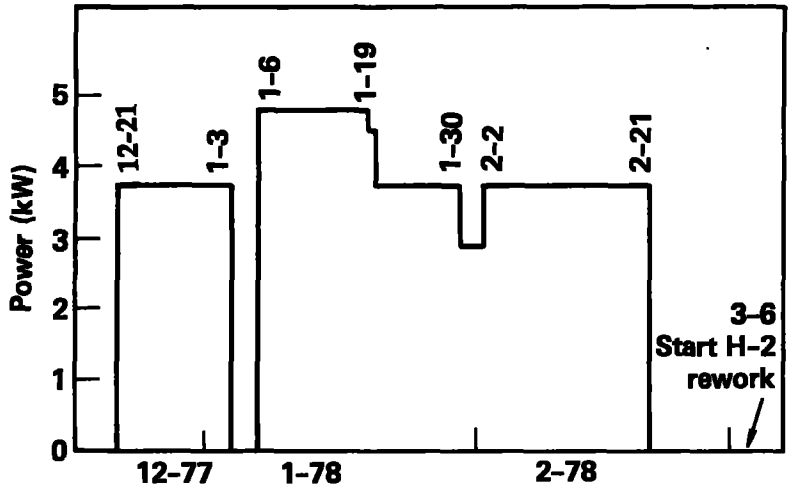

Figure 10. Power history of H-2.

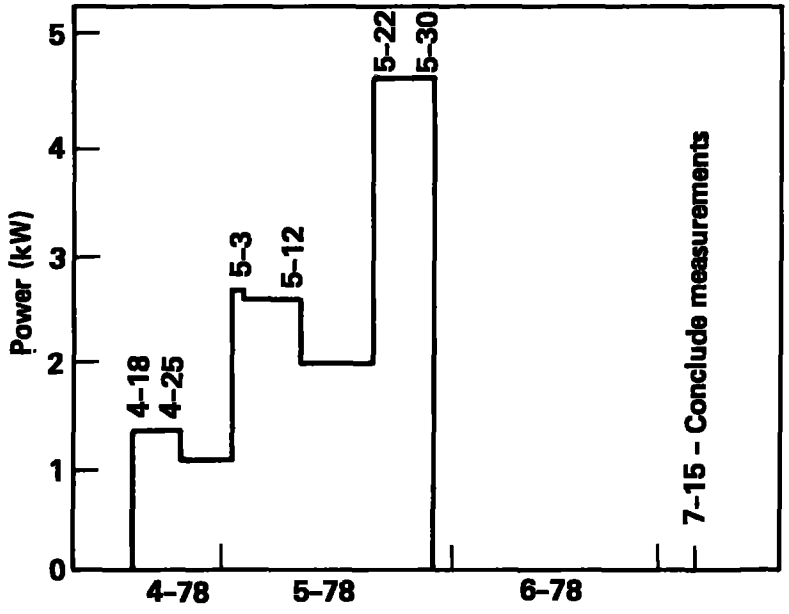

Figure 11. Power history for permeability test.

Data Analysis

Heater Tests

Our data analysis for the heater tests consisted primarily of comparing the measured and calculated temperature histories of selected thermocouples. To make the comparison, we varied the conductivity and diffusivity in the calculations until reasonable agreement between the measured and calculated temperatures was attained.

The calculational technique used was basically simple, namely the superposition in space and time of the continuous point-source solution of the diffusion equation

$$\Delta T = \frac{Q}{4\pi k d} \operatorname{erfc} \sqrt{\frac{d^2}{4\kappa t}},$$

where

ΔT = temperature rise (K)
Q = source strength (W)
d = distance from point source (m)
k = thermal conductivity (W/m·K)
κ = thermal diffusivity (m^2/s)
t = time (s)
erfc = complementary error function

We used a sufficiently large number of poin sources to represent each finite-length heater so

at a distance corresponding to the nearest instrument holes, the combined solutions were essentially identical with that of a line-segment source. The material surrounding the heater was assumed to be isotropic, with constant thermal conductivity and thermal diffusivity independent of temperature. For each heater test, we used the power history (i.e., Fig. 9 or 10) to determine appropriate values of Q for the duration of each heating segment. Then we performed one calculation for each trial set of k and κ values. That is, the above formula has a fixed value of Q for each time period of fixed heater power; thus, temperature histories can be evaluated at any desired set of distances (d) from the source by summing the contributions of all point sources used to simulate the heater. Using superposition in time, we combined the solution for each constant-power heating segment with the other constant Q solutions to complete one full calculation for each trial set of k and κ. Such calculations were used to produce temperature histories at distances corresponding to each thermocouple location.

Heater Test Results

The unplanned power loss during the H-1 test was most useful for data analysis. The temperature minimum at about 295 h proved to be the most sensitive region for purposes of comparison, especially for diffusivity. Figures 12 to 14 show a comparison of data and calculations for a 20-h time span centered about the minimum. The data shown in these figures are from the two midplane thermocouples in hole I-02 (~0.5 m from the heater). These measurements were made in a plane parallel to the principal fracture orientation (Fig. 2).The calculations show the sensitivity of the temperature of the medium to variations in conductivity, diffusivity, and location (any uncertainty in heater power would affect the results inversely as a variation in conductivity). As expected, small changes in conductivity show a linear shift in temperature, while variations in diffusivity (which affects the time constant) show a shift in minimum temperature time and a crossover in calculated temperature following the minimum. While a change in position shows a shift in temperature, the shift tends to be stronger during the heating phase than during cooling. Because the data show the same tendency, we suspect that the two thermocouples were not at the same radial position from the heater, but differed by a few millimeters because of rotation of the assembly during installation.

On the basis of the results of the sensitivity study described above, we used the values k = 3.08 W/m·K for thermal conductivity and κ = 1.21 mm^2/s for thermal diffusivity to calculate temperature-rise-vs-time histories for each thermocouple location. Plots of these calculations and the measured temperature rises are shown in Appendix A. The letter designations indicate locations below the heater midplane (A), at the midplane (B and C), and above the midplane (D).

Agreement between the calculations and measurements varies. The worst cases are those in which the calculated temperature goes above the boiling point of water (a temperature rise of ~73°C over the ambient temperature of ~23°C). In these cases, water—probably from residual drilling fluid—boils and the resulting steam rises, condenses to liquid water in a cooler region, and runs back to be boiled again. The result is a reflux zone clamped at the boiling point, or a heat pipe transferring heat from the bottom of the zone to the top.

When and where boiling water effects were not important, the heater test data appear to fit with values near k = 3.1 W/m·K for thermal conductivity and κ = 1.2 mm^2/s for thermal diffusivity. As noted above, these values were obtained from measurements in the plane parallel to the principal fracture direction. We observed that the level of agreement between measured and calculated temperature histories is nearly as good in the orthogonal direction. For example, compare I-01 (p. A-3) with I-11 (p. A-9) and I-03 (p. A-6) with I-09 (p. A-12). Since errors in temperature rise are inversely proportional to errors in conductivity, we conclude that the anistropy in the thermal properties of the rock is on the order of a few percent. These results are consistent with other measurements for granitic rock at the Nevada Test Site. In 1960 the U.S. Geological Survey reported on the thermal conductivities of 14 core samples from the U15a No. 31 exploration hole.[7] These samples, taken from a depth of 19 to 366 m, had an average value of 2.62 W/m·K, with a standard deviation of 0.31. In 1982 Durham[8] reported on the measurements of three samples, one from the H-2 hole and two from a hole ~75 m to the southwest. He gives thermal conductivity and diffusivity values as k = 2.75 ± 0.25 W/m·K and κ = 1.25 ± 0.4 mm^2/s, respectively. While the mean conductivity may appear to be significantly different than the value we determined here (3.08

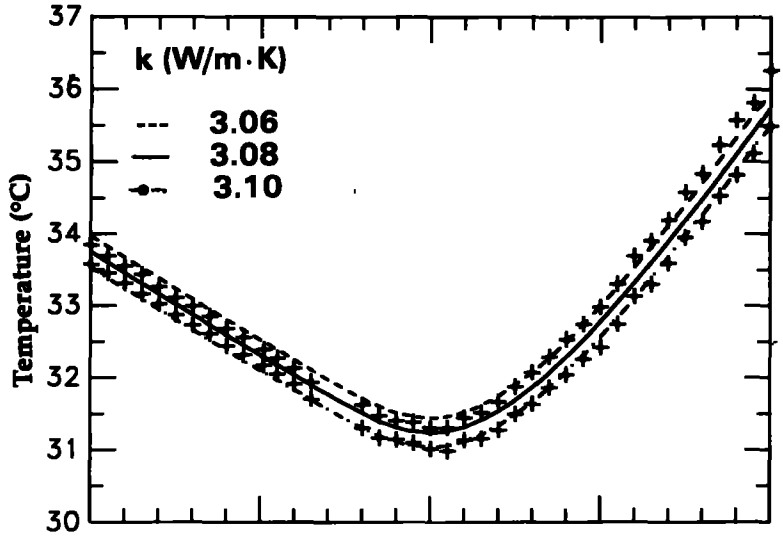

Figure 12. Measured and calculated data for 20-h time span from tw midplane thermocouples in hole I-02 showing sensitivity with respect to conductivity. Here κ = 1.21 mm^2/s and R = 499 mm.

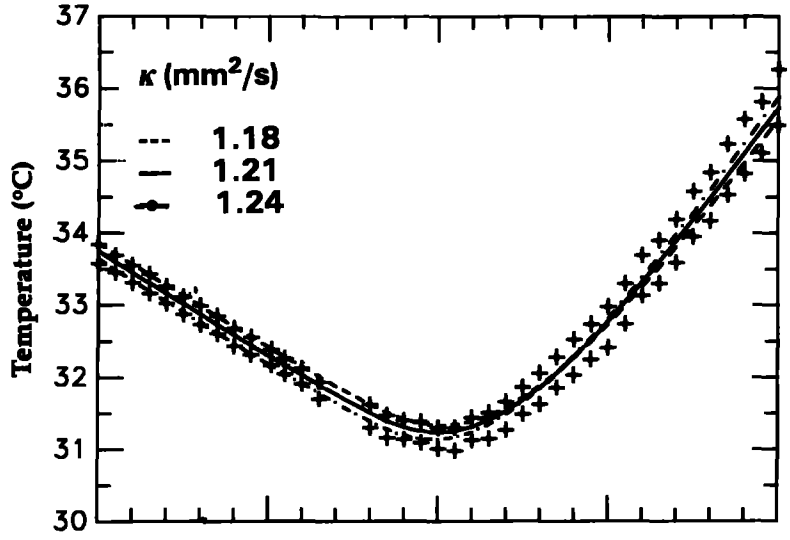

Figure 13. Measured and calculatec data for 20-h time span from tw midplane thermocouples in hole I-02 showing sensitivity with respect to diffusivity. Here k = 3.08 W/m·K anc R = 499 mm.

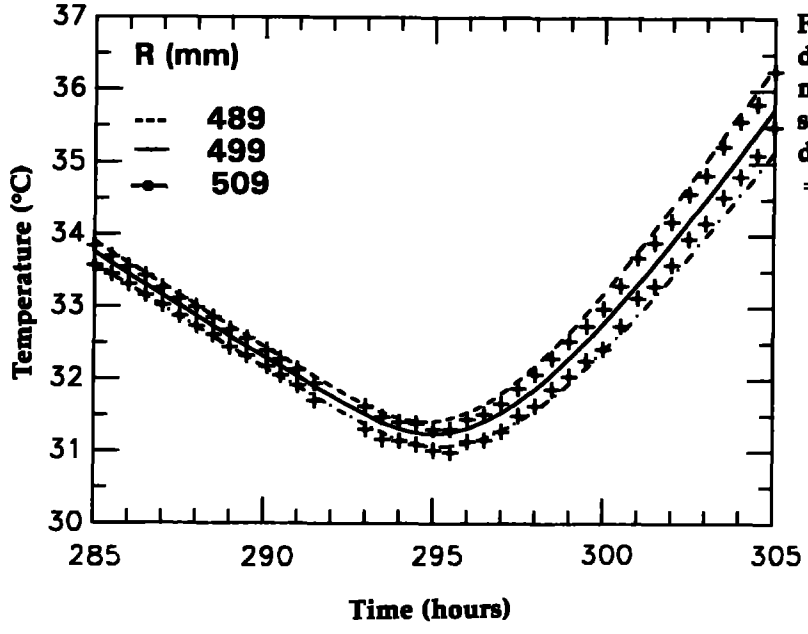

Figure 14. Measured and calculate data for 20-h time span from tw midplane thermocouples in hole I-0 showing sensitivity with respect tc distance. Here k = 3.08 W/m·K and = 1.21 mm^2/s.

W/m·K), examination of Durham's (Durham 1982) data shows that this is not the case. Conductivities cluster near 2.6 W/m·K for one sample and near 3.0 W/m·K for the other. Given the small sample size and known heterogeneity of the granite, such variability is anticipated. The in-situ measurements are a more accurate reflection of the average over a large volume.

Permeability Data Analysis

The data analysis for the permeability test was based on Jaeger's (1956) solution for the cooling of a heated infinite cylinder. His power series expansion,[9] when written in terms of fluid flow in a porous medium for the pressure decay in an infinite cylindrical hole with an initial pressure P_0 in a homogeneous isotropic medium, is

$$\frac{P}{P_0} = 1 - \frac{4}{\sqrt{\pi}}\phi\,\tau^{1/2} + \phi(4\phi - 1)\tau + \text{terms } 0\left(\tau^{3/2}, \text{etc.}\right)$$

or

$$\frac{P}{P_0} = 1 - \frac{4}{\sqrt{\pi}}\phi\,\tau^{1/2} - \phi\tau \text{ for small } \phi \text{ and } \tau,$$

where

P = pressure in cylindrical hole (Pa)
ϕ = porosity
τ = t/t_c
t = time elapsed (s)
t_c = time constant = r^2/κ (s)
r = radius of hole (m)
κ = diffusivity ($\bar{P}k/\phi\mu$) (m^2/s)
$\bar{P}$ = mean pressure (Pa)
k = permeability (m^2)
μ = viscosity (Pa·s)

The use of a pure radial-flow solution (infinite cylinder) seems intuitively reasonable because of the high length-to-diameter ratio (~60) of the packed-off section of the holes. The error introduced by the radial-flow assumption is of interest and has received considerable study in the analogous field of using probe methods to determine the thermal properties of materials in bulk. Following Blackwell (1953),[10] we find the relative error in the calculated pressure is approximately erfc ($\lambda/2\sqrt{\tau}$), where λ is the length-to-diameter ratio. For most of our permeability measurements, the value of τ at the end of the measurement was in the range 1 to 10, giving a negligible error. In only one case (P-01, run S) was τ large (~300). This indicates a relative error of only 0.015.

Adapting the linear form of the diffusion equation (applicable to heat flow) to the inherently nonlinear problem of porous flow of a compressible gas requires some attention. A common way to "linearize" the gas-flow problem is to use $\bar{P} = (P_{max} + P_{min})/2$, particularly when the pressures are not too different. In our case, however, the pressure ratio $P_0/P_{ambient} = N \sim 10$, and further consideration seemed prudent.

To better approximate $\bar{P}$, we considered a related problem of one-dimensional Cartesian flow in a semi-infinite medium having a constant pressure boundary. This problem was first studied by Wagner (1950)[11] in terms of nonlinear chemical diffusion. His results are equivalent to the pressure ratio $N = \infty$. Morrison (1972)[12] studied the same problem and extended the solutions to finite N. The problem can be solved numerically, using only two variables for a given N, by Boltzmann's similarity transformation. The results may be expressed as

$$\Phi = f(\theta, N),$$

where Φ is a dimensionless pressure or concentration and the space–time variable θ is given (using Morrison's formulation) by

$$\theta^2 = \frac{X^2\phi\mu}{4kt\Delta P}.$$

We can compare this solution to the linearized solution of the diffusion equation for the same geometry. If we use the linear form of the diffusion equation and replace ΔP with $\bar{P}$, the solution is

$$\Phi_{lin} = \text{erfc}\,(\theta_{lin})$$

To obtain a usable approximation for $\bar{P}$, we match the linear and nonlinear solutions at the boundary ($\theta = 0$). Because the solutions are normalized to one at $\theta = 0$, we have the first derivatives at our disposal. Thus, the linear and nonlinear solutions will agree in both value and flow rate at the surface if we set

$$\frac{\left(\frac{d\Phi}{d\theta}\Big|_{\theta=0}\right)_{lin}}{\theta_{lin}} = \frac{\left(\frac{d\Phi}{d\theta}\Big|_{\theta=0}\right)_{N}}{\theta_N},$$

giving

$$\tilde{P} = \Delta P \left. \frac{\left(\frac{d\Phi}{d\theta}\right)^2_N}{\left(\frac{d\Phi}{d\theta}\right)^2_{lin}} \right|_{\theta=0}$$

From the properties of the error function, we have

$$\left(\frac{d\Phi}{d\theta}\right)_{lin} = -\frac{2}{\sqrt{\pi}}$$

and from Morrison[13]

$$\left(\frac{d\Phi}{d\theta}\right)_{N=10} = -0.86985,$$

both calculated at $\theta = 0$. This adjusts our approximation for $\tilde{P}$ to

$$\tilde{P} = \frac{\Delta P}{1.68}$$

instead of the $\tilde{P} = \Delta P_{ave}$ sometimes used for linearized problems. We then use this "adjusted" value of $\tilde{P}$ in the linearized solution for the infinite cylinder. This allows us to include the effects of radial flow that were not included in the nonlinear solution for the planar problem.

In the above discussion of test sequences we mentioned that the ideal permeability test would be conducted at constant temperature so that pressure change in the hole would be due entirely to fluid flow into the drill-hole walls. By adjusting the power levels just before each pressurization test, we obtained nearly constant temperatures when the heater was operational. Figure 15 shows a temperature curve for a pressurization test hole located 0.4 m from the heat source. This curve is representative of the temperature histories in all of the pressurized holes. The seven pressurization tests are indicated in Fig. 15 by letter designations M through S. The length of each pressurization cycle and the change in temperature that occurred during each test can also be seen in Fig. 15. During tests M, N, and O, relatively constant temperatures were achieved, as planned. After the heater failed, P experienced large changes in pressure and, thus, failed to yield usable data. Subsequent tests during the cooling portion of the history (tests Q, R, and S) were close enough to constant temperature that temperature corrections to the hole pressure lead, by the above formula, to a usable interpretation of the pressure decay.

For each pressurization test, we took the pressure at any time in each hole and "corrected" it to

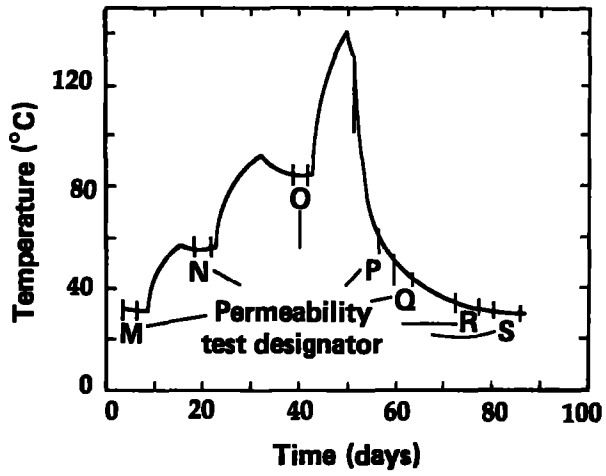

Figure 15. Temperature history of permeability test at 0.4 m from heater.

what it would have been at the starting temperature. We did this by multiplying the pressure by the ratio of the absolute temperature at a given time to the starting temperature in that hole. That is, we assumed an equation-of-state linear with absolute temperature for the air pressurizing the hole, such as the ideal gas equation $P = nRT/V$. The temperatures for this correction were obtained by averaging the values for the four thermocouples in each pressurization test hole. The "corrected" pressures, P, were then plotted as P vs $\sqrt{t}$ and fit, using standard least-squares techniques, to a function of the form

$$P = P_0 + P_1\sqrt{t} + P_2 t ,$$

giving as a parabola the P vs $\sqrt{t}$ curve. The resulting parabolic curves, together with the actual data used to obtain the least-squares fit, are shown in the upper half of each figure in Appendix B. In each of the least-squares fits to the data, the first few pressure points obtained immediately after pressurization did not lie on the best-fit parabola for the remainder of the data. Yet, the remainder of the data was extremely close to a parabola. This effect of the first few points not lying on the best-fit parabola becomes clearer if we rearrange the above formula and plot the data in a form that should result in a straight line:

$$\frac{1 - \frac{P}{P_0}}{\sqrt{t}} = A + B\sqrt{t} .$$

Then, if the data for each pressurization test are plotted as $(1 - P/P_0)/\sqrt{t}$ vs $\sqrt{t}$ and the pressure decays according to the approximation used, the resulting curve should be a straight line. The bottom figures in Appendix B show both the straight-line fits to the data and the data used for each pressurization test in each hole. In these plots one can easily see that the early-time points (for about the first hour after pressurization) are usually badly scattered. After the first hour, however, the data are quite close to linear for most of the holes. We interpreted this nonlinear behavior during the first hour as the result of disturbances in both the temperature and stress state caused by the sudden injection of ~100-psi air at ambient temperature. Thus, we usually avoided using these first few data points in the data fit for the best straight line through the pressure decay data.

Our data-reduction program allows the user to specify some number of points at the beginning and/or end of the data that are to be ignored in the curve fitting. It also allows the user to select a tolerance level, in standard deviation units, for the data points to be accepted. All data are shown in the plot as circles (to be ignored) and crosses (to be used). In the plots in Appendix B the first 14 points and any point exceeding 2.5 sigma are ignored. Appendix B contains the data for and analysis of all sets that gave meaningful results. It also contains the data and analysis for test O, hole J-02 (Fig. B-10), which shows a typical bad result. Here, the noise in the data (although small) is greater than the total pressure drop and leads to negative permeability and porosity. By contrast, test O, hole H-2 (Fig. B-9), the only heater hole data to show positive results, has more than five times as much scatter in the data (presumably the result of temperature fluctuations caused by fluctuations in line voltage), but a much greater pressure drop.

We calculated the permeability and porosity from the values obtained for A and B in the best-fit straight line:

$$k = \frac{r^2\mu}{P} B$$

and

$$\phi = \frac{\pi A^2}{16B},$$

where $r = 24$ mm and $\mu = 1.75 \times 10^{-5}$ Pa·s.

The constants A and B were calculated from the constants P_0, P_1, and P_2 of the quadratic least-squares fit.

Permeability Test Results

Table 2 is a summary of the average permeabilities obtained in the various pressurization tests. Included are the average permeabilities, porosities, temperatures, and root-mean-square residuals resulting from the curve fitting. The residuals are generally well below the manufacturer's stated transducer repeatability of 0.3 psi.

Note that the permeability values are substantially different from those reported previously.[3] This is a result of the improved analysis method described above. The permeability obtained at ambient temperature was approximately 1 nD. At about 50°C above ambient (during heating), the permeability decreased to 0.2 nD; at higher temperatures, it became too small to measure (<0.02 nD). Upon subsequent cooling, the permeability returned to approximately its preheat value of 1 nD. The ambient-temperature permeabilities of regions that had been thermally cycled to high temperatures before the pressurization tests (i.e., during the heater tests) were approximately the same as those in regions that had not undergone thermal cycling.

Conclusions

The in-situ conductivity value of 3.1 W/m·K obtained from the heater tests is consistent with other measures in Climax Stock granite. The in-situ diffusivity was approximately 1.2 mm²/s. Anisotropic effects in the thermal field were less than 10%. The good agreement between the calculated and experimental temperature histories for all thermocouple stations using the above values for k and κ gives credence to the results of analyses using similar values to predict the thermal fields resulting from emplaced nuclear waste and heaters at the Spent Fuel Test—Climax.[1]

Our heater tests provided valuable lessons on how to obtain good thermal data in situ. In par-

Table 2. Permeability test results (see Fig. 15 for test sequence designator).

Borehole designator	Distance (m)[a]	M		N		O		P		Q		R		S	
H-2	0.0	b 32.4	b 0.016	b 290.9	b 0.049	1.09 419.3	0.0071 0.082	b 85.0	b 0.261	PF		PF		PF	
J-02	0.4	0.40 32.3	0.0028 0.007	0.15 51.2	0.0010 0.009	b 74.3	b 0.015	PF		PF		PF		PF	
I-09	0.73	0.62 32.4	0.0047 0.007	0.13 43.6	0.0103 0.007	b 59.4	b 0.014	0.070 70.9	0.0029 0.060	0.93 46.8	0.0011 0.009	1.08 36.4	00018 0.008	NI	
I-10	0.37	1.19 32.4	0.0031 0.007	0.24 53.4	0.0053 0.017	b 78.4	b 0.062	b 80.8	b 0.043	0.78 47.7	0.0013 0.008	1.16 36.6	0.0009 0.009	NI	
I-11	0.4	0.69 32.3	0.0001 0.009	0.13 51.3	0.0012 0.018	b 74.1	b 0.067	b 78.8	b 0.077	1.03 47.5	0.0025 0.008	1.27 36.5	0.0013 0.007	1.31 33.7	0.0010 0.009
I-06	4.92	NI		NI		NI		NI		NI		NI		0.88 28.7	0.0013 0.010
P-01	5.23	NI		NI		NI		NI		NI		NI		1.67 28.2	0.0001 0.015

Perm., k, nD	Porosity, ϕ
Temp., t, °C	Residual error, psi

[a]Distance to test borehole measured from centerline of heater borehole.
[b]No meaningful result. Negative permeability and porosity calculated.
NI = not instrumented.
PF = packer failure.

ticular, they reinforced our intuition that the earth itself provides a more stable temperature reference than expensive commercial gadgets. In general, we found that the thermocouples and pressure gauges were more accurate than the manufacturer's conservative specifications, which are based on interchangeability requirements. For example, the specifications referred to absolute temperature values that were only accurate to ±2°C, but we found that temperature *changes* of a few hundredths of a degree were consistently detected and reproduced in our analysis of the temperature histories. We also learned that data-reduction programs should be operational before in-situ measurements are taken so that a feedback of results is immediately available. The kind of data analysis used in these tests can tolerate *natural* self-cycles (such as heater failure) while providing data that are just as useful and valid as those obtained from planned *ideal* test sequences.

The permeability of the granite was low at ambient temperature (~1 nD), and thermal cycling did not cause significant changes in its permeability. After high-temperature (~150°C) excursions, the permeability was approximately the same as that measured in rock that had never been heated. We could interpret the significant decrease in this already low apparent permeability with increasing temperature as implying that the permeability of the intact rock was essentially zero, with the actual pressure decay in the tests being due primarily to the fracture (or microfracture) flow of the gas. However, we know that the increasing temperature causes increasing compressive stresses in the surrounding rock, closing the available fractures and, thus, causing the apparent permeability to decrease significantly as the fractures close.

Acknowledgments

This project was sponsored initially by the Energy Research and Development Agency and then by the Department of Energy, Office of Nuclear Waste Isolation, through the Nevada Operations Office. We wish to thank these sponsoring agencies for their continuous support of the project.

Our thanks also go to the many individuals who worked on or contributed to the project. Special acknowledgments go to L. D. Ramspott, Waste Isolation Projects Manager at LLNL, to L. B. Ballou, who provided overall technical leadership and assisted with the data reduction and analysis, to W. G. Brough for the design, fielding, and survival of the data-acquisition system, to O. R. Walton for reviewing and assisting with the editing of parts of this report, and to the late F. A. Morrison, Jr., for helpful discussions relating to the permeability data analysis.

References

1. D.N. Montan and W. Patrick, *Thermal Calculations for the Design, Construction, Operation, and Evaluation of the Spent Fuel Test—Climax, Nevada Test Site,* Lawrence Livermore National Laboratory, Livermore, CA, UCRL-53238 (1981).
2. L. D. Ramspott, Ed., *Waste Isolation Projects—FY1977,* Lawrence Livermore National Laboratory, Livermore, CA, UCRL-50050-77 (1978).
3. L. D. Ramspott, Ed., *Waste Isolation Projects—FY1978,* Lawrence Livermore National Laboratory, Livermore, CA, UCRL-50050-78 (1979).
4. L. D. Ramspott, *Climax Granite Test Results,* Lawrence Livermore National Laboratory, Livermore, CA, UCID-18502 (1980).
5. L. B. Ballou, *Geological Disposal Investigations in Granite at the Nevada Test Site,* Lawrence Livermore National Laboratory, Livermore, CA, preprint UCRL-82284 (1979).
6. W.L. Ellis and J.E. Magner, *Determination of the In Situ State of Stress at the Spent Fuel Test Climax Site, Climax Stock, Nevada Test Site,* U.S. Geological Survey, Open File Report 82-458 (1982).
7. G. A. Izet, *Granite Exploration Hole, Area 15, Nevada Test Site, Nye County, Nevada—Interim Report, Part C, Physical Properties,* U. S. Geological Survey, TEM-836-C (1960).

8. W. B. Durham, *Thermal Properties of Climax Stock Quartz Monzonite to 523 K and 50-MPa Confining Pressure*, Lawrence Livermore National Laboratory, Livermore, CA, UCRL-53349 (1982).
9. J. C. Jaeger, "Conduction of Heat in an Infinite Region Bounded Internally by a Circular Cylinder of a Perfect Conductor," *Aust. J. Phys.* **9**, 167–179 (1956).
10. J. H. Blackwell, "Radial–Axial Heat Flow in Regions Bounded Internally by Circular Cylinders," *Can. J. Phys.* **31**, 472 (1953).
11. C. Wagner, "Diffusion of Lead Chloride Dissolved in Solid Silver Chloride," *J. Chem. Phys.* **18**, 1227 (1950).
12. F. A. Morrison, Jr., "Transient Gas Flow in a Porous Column," *Ind. Eng. Chem. Fundam.* **11**, 191 (1972).
13. F. A. Morrison, Jr., Lawrence Livermore National Laboratory, Livermore, CA, private communication (1983).

Appendix A
Heater Test Data and Calculations

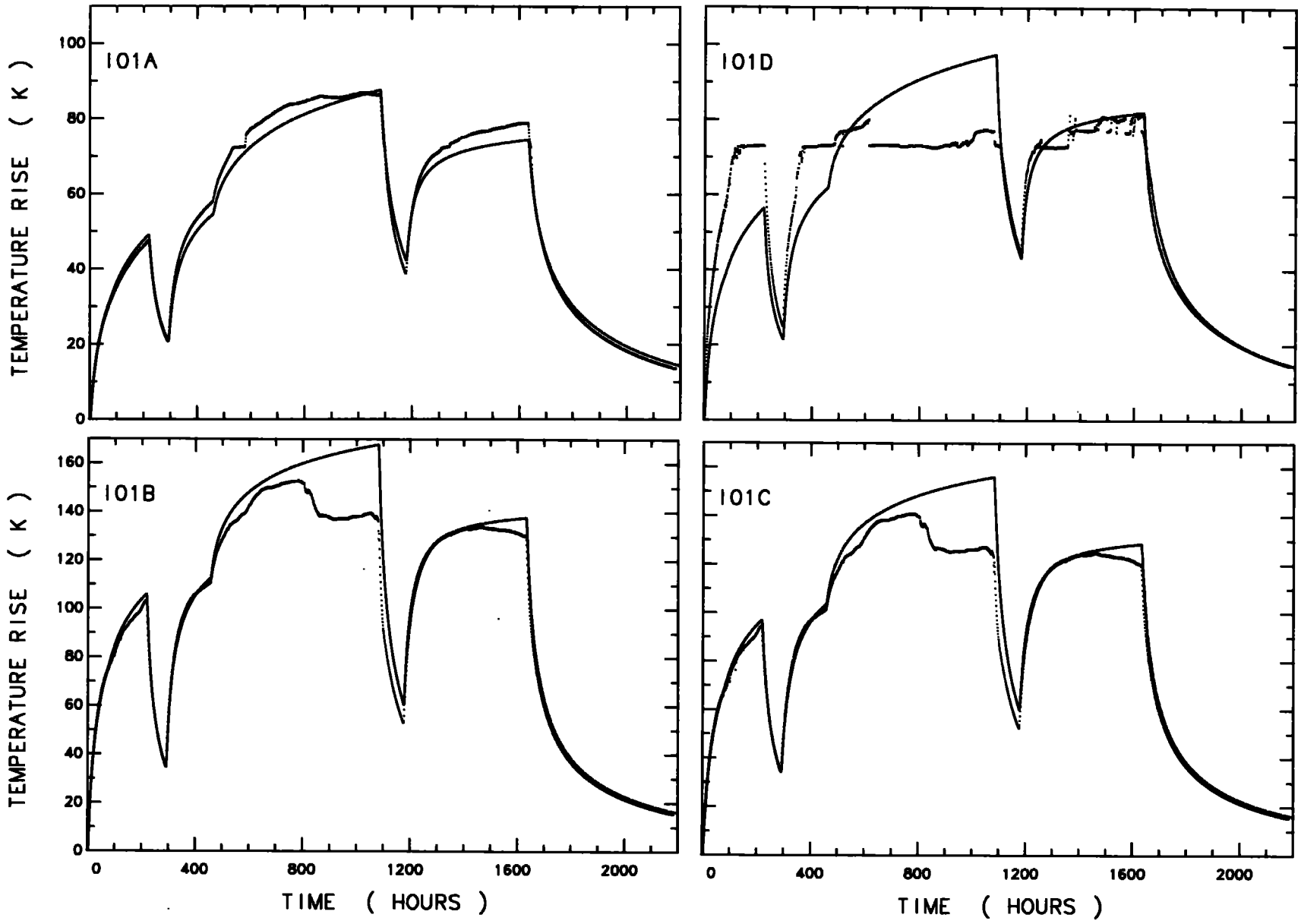

Figure A-1. Calculated and measured temperature histories for test using heater H-1, borehole I-01. Alphabetic codes are A = below heater, B and C = at heater midplane, and D = above heater midplane.

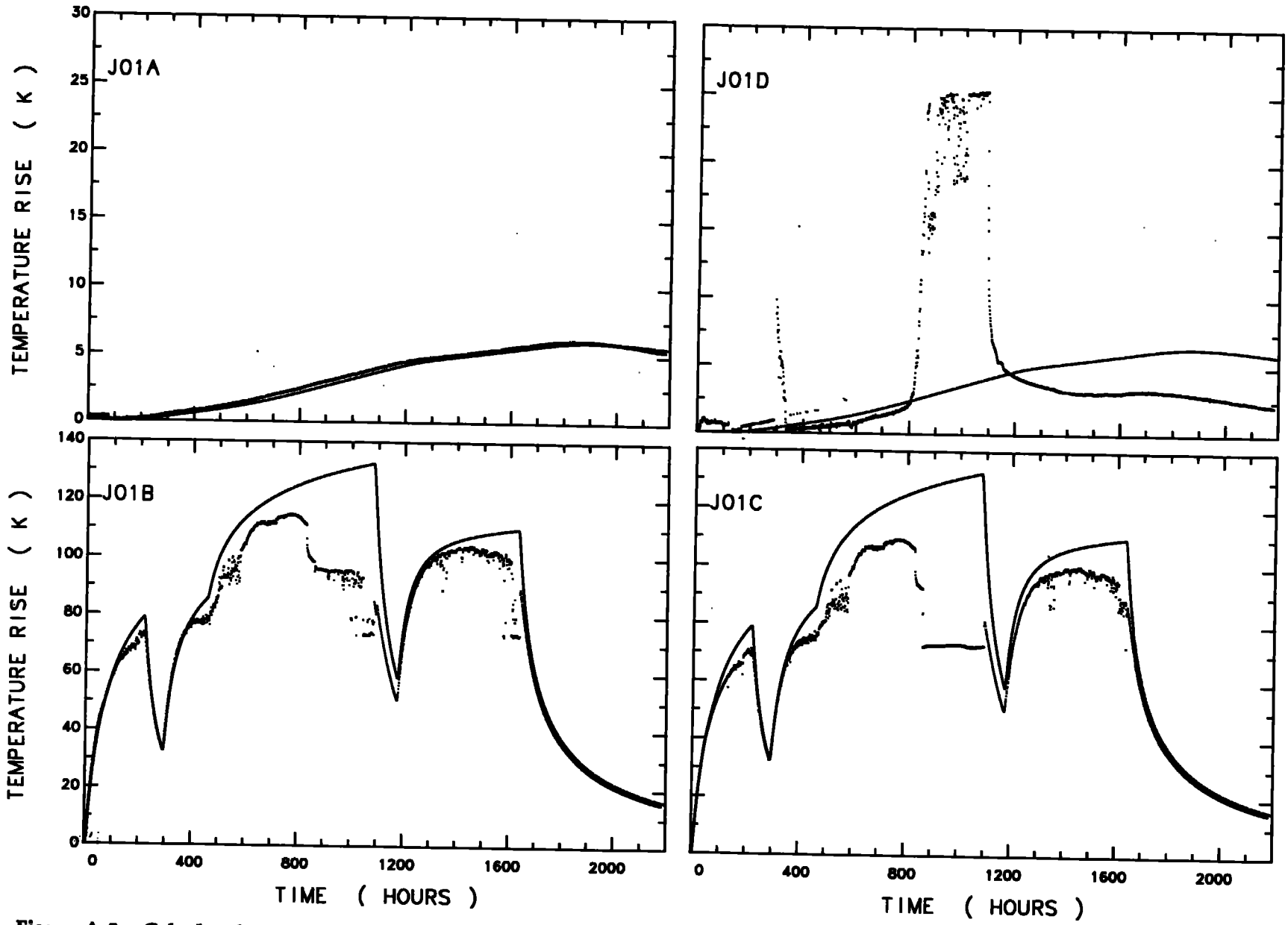

Figure A-2. Calculated and measured temperature histories for test using heater H-1, borehole J-01. Alphabetic codes are A = below heater, B and C = at heater midplane, and D = above heater midplane.

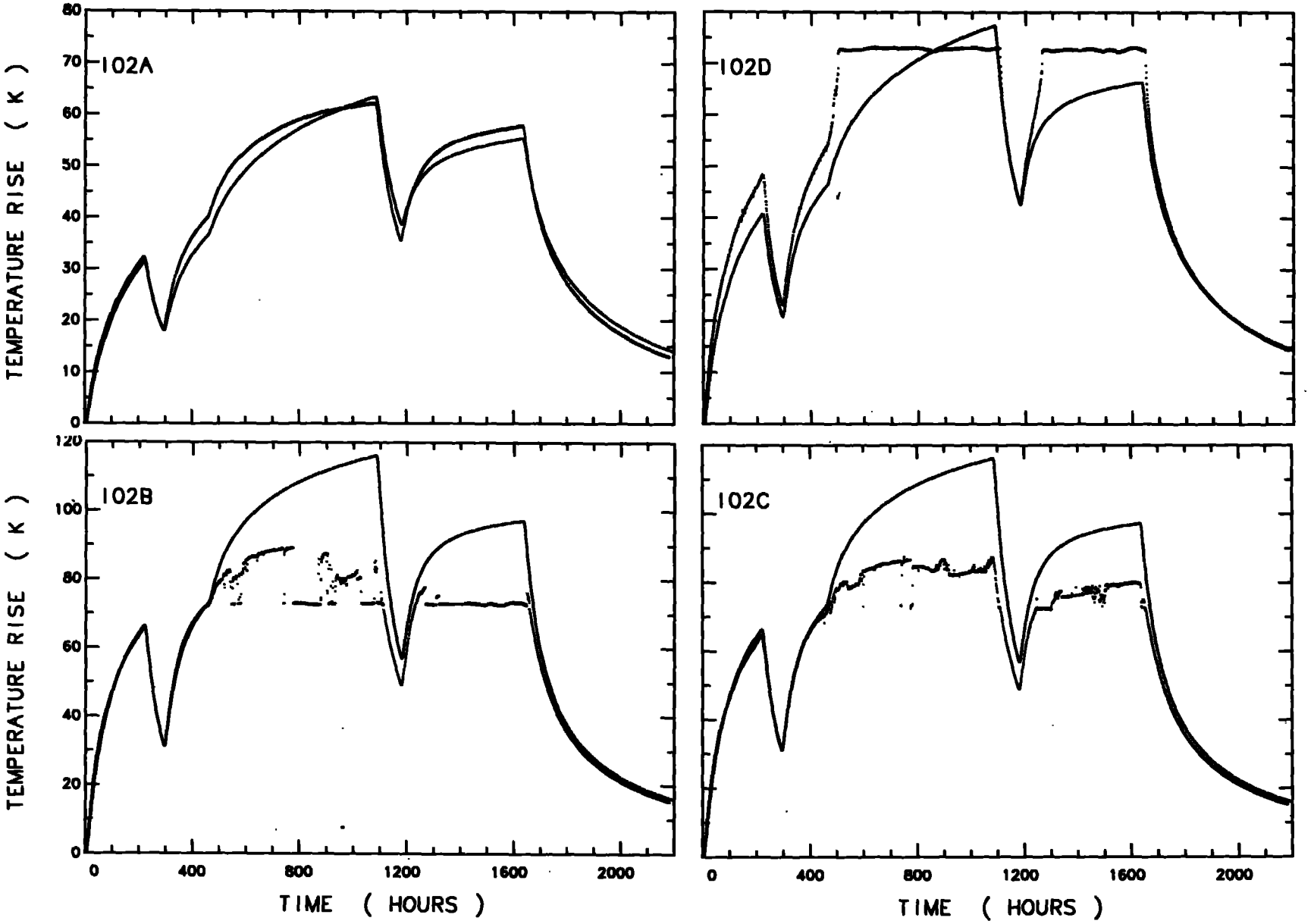

Figure A-3. Calculated and measured temperature histories for test using heater H-1, borehole I-02. Alphabetic codes are A = below heater, B and C = at heater midplane, and D = above heater midplane.

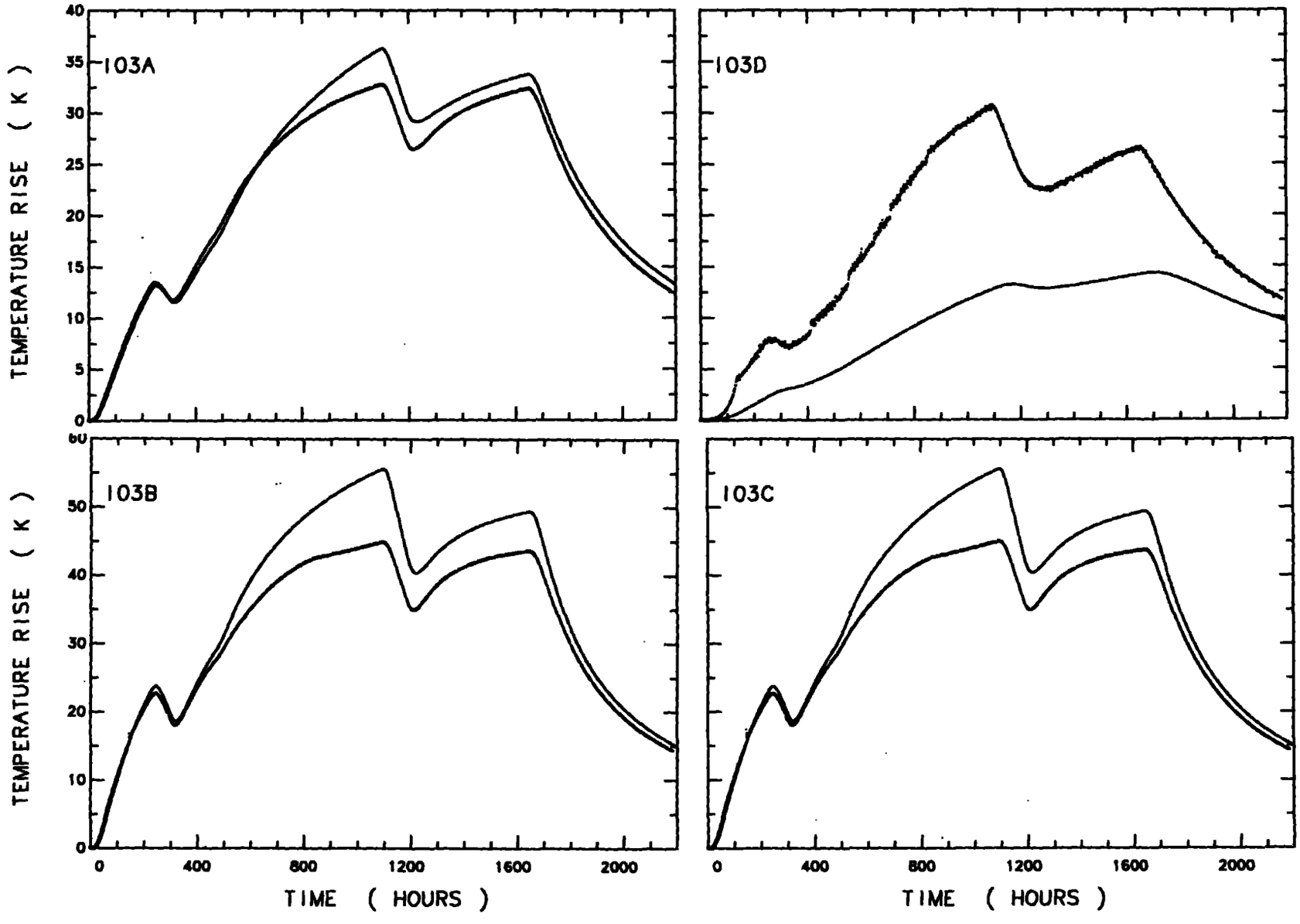

Figure A-4. Calculated and measured temperature histories for test using heater H-1, borehole I-03. Alphabetic codes are A = below heater, B and C = at heater midplane, and D = above heater midplane.

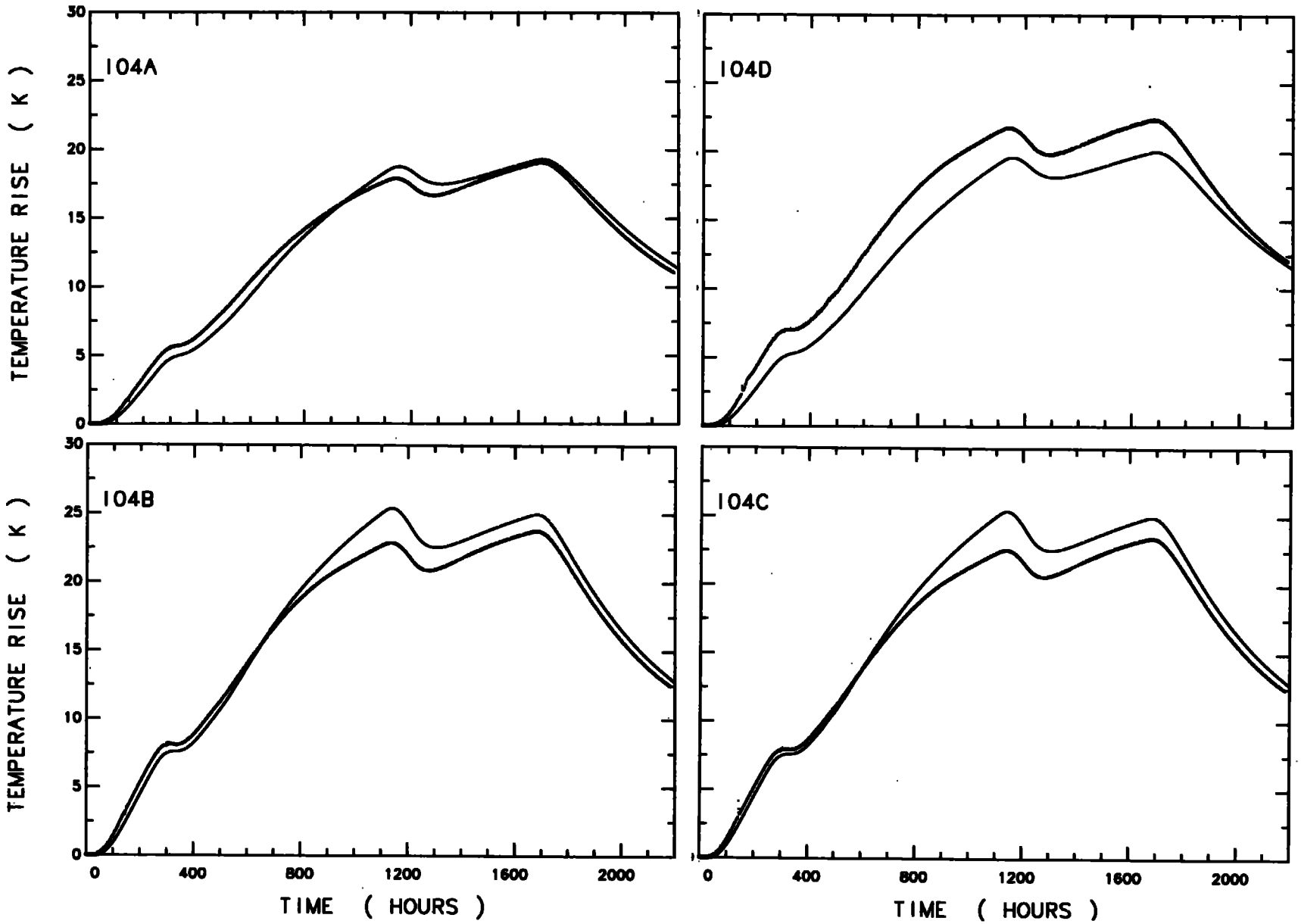

Figure A-5. Calculated and measured temperature histories for test using heater H-1, borehole I-04. Alphabetic codes are A = below heater, B and C = at heater midplane, and D = above heater midplane.

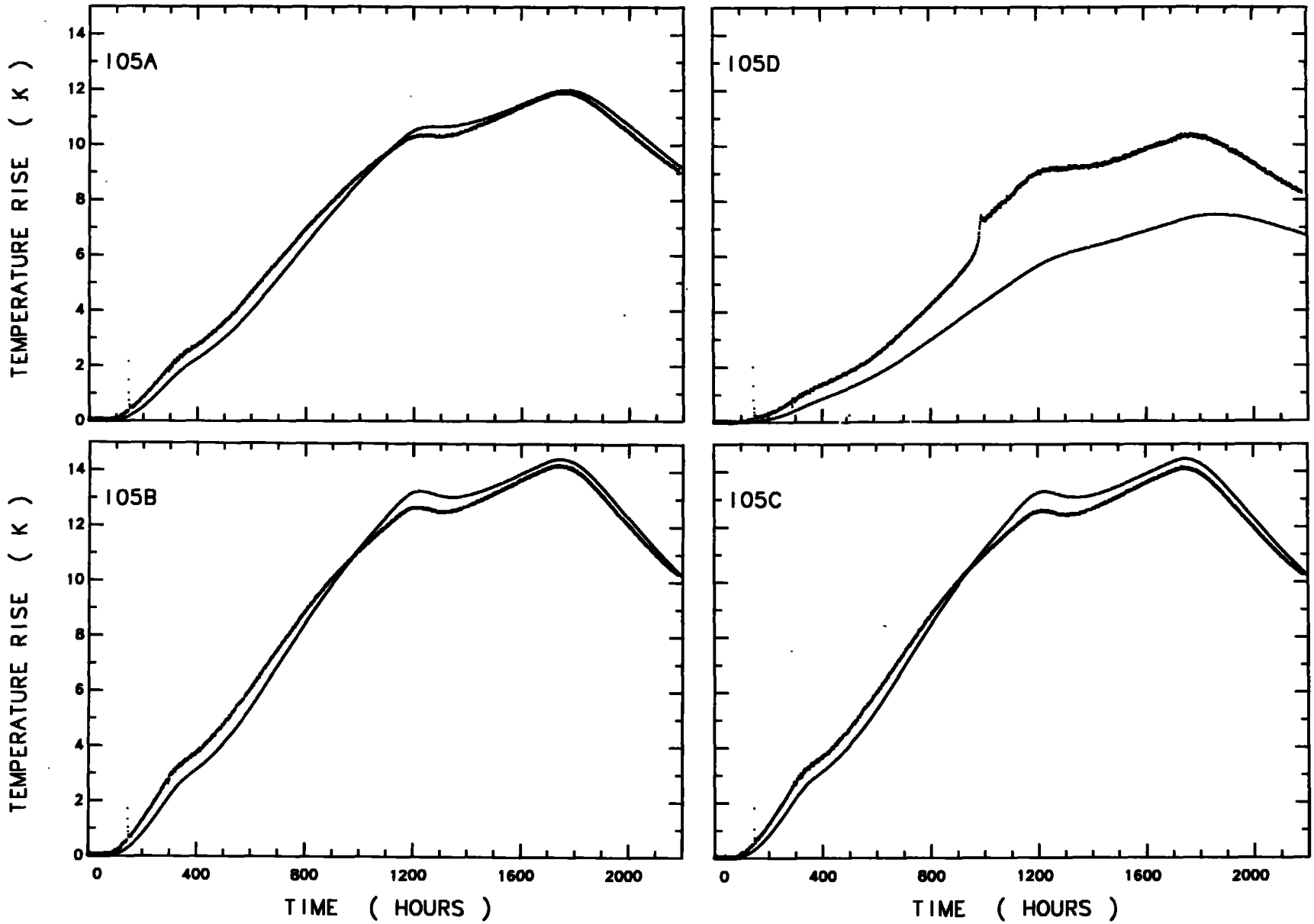

Figure A-6. Calculated and measured temperature histories for test using heater H-1, borehole I-05. Alphabetic codes are A = below heater, B and C = at heater midplane, and D = above heater midplane.

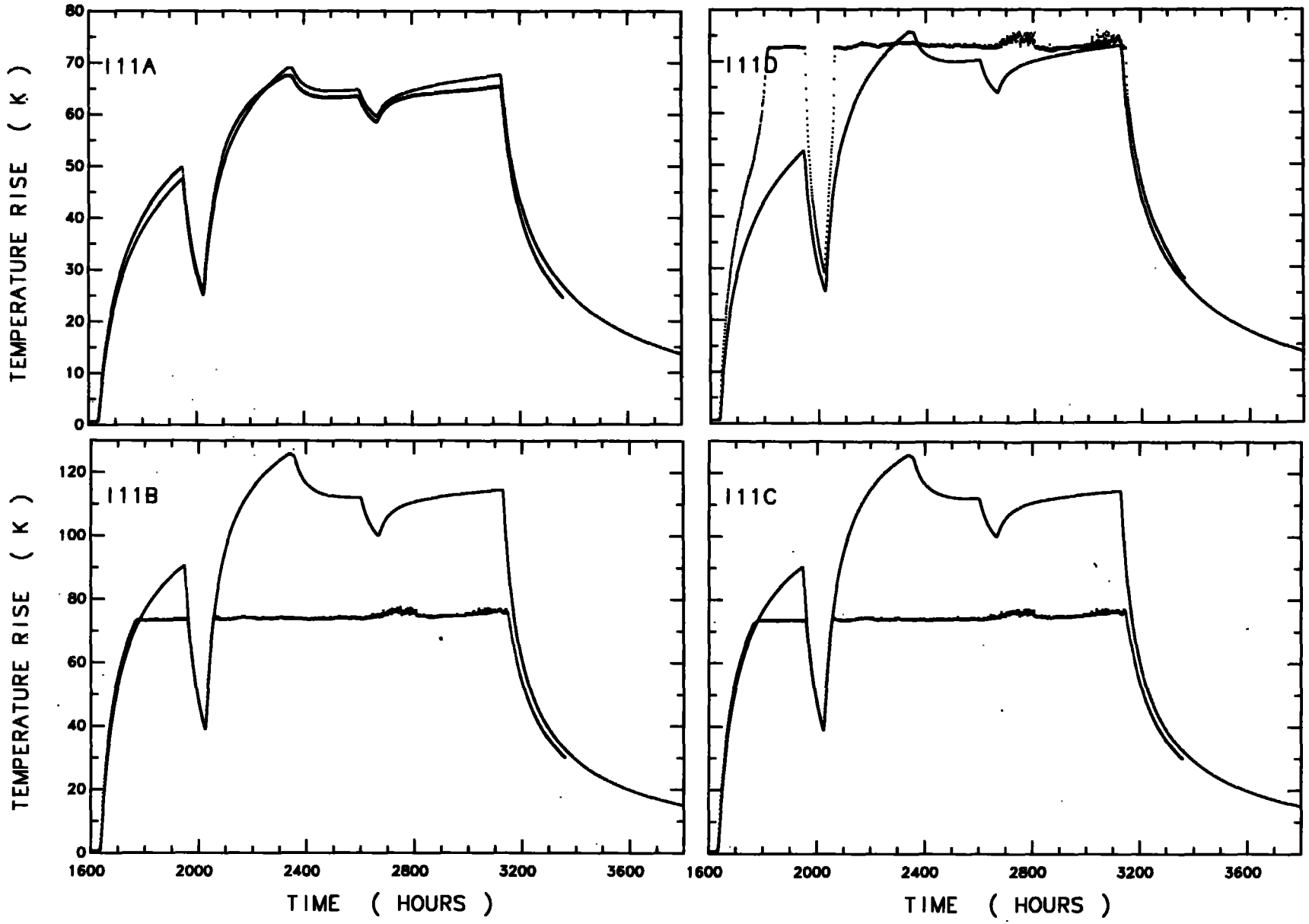

Figure A-7. Calculated and measured temperature histories for test using heater H-2, borehole I-11. Alphabetic codes are A = below heater, B and C = at heater midplane, and D = above heater midplane.

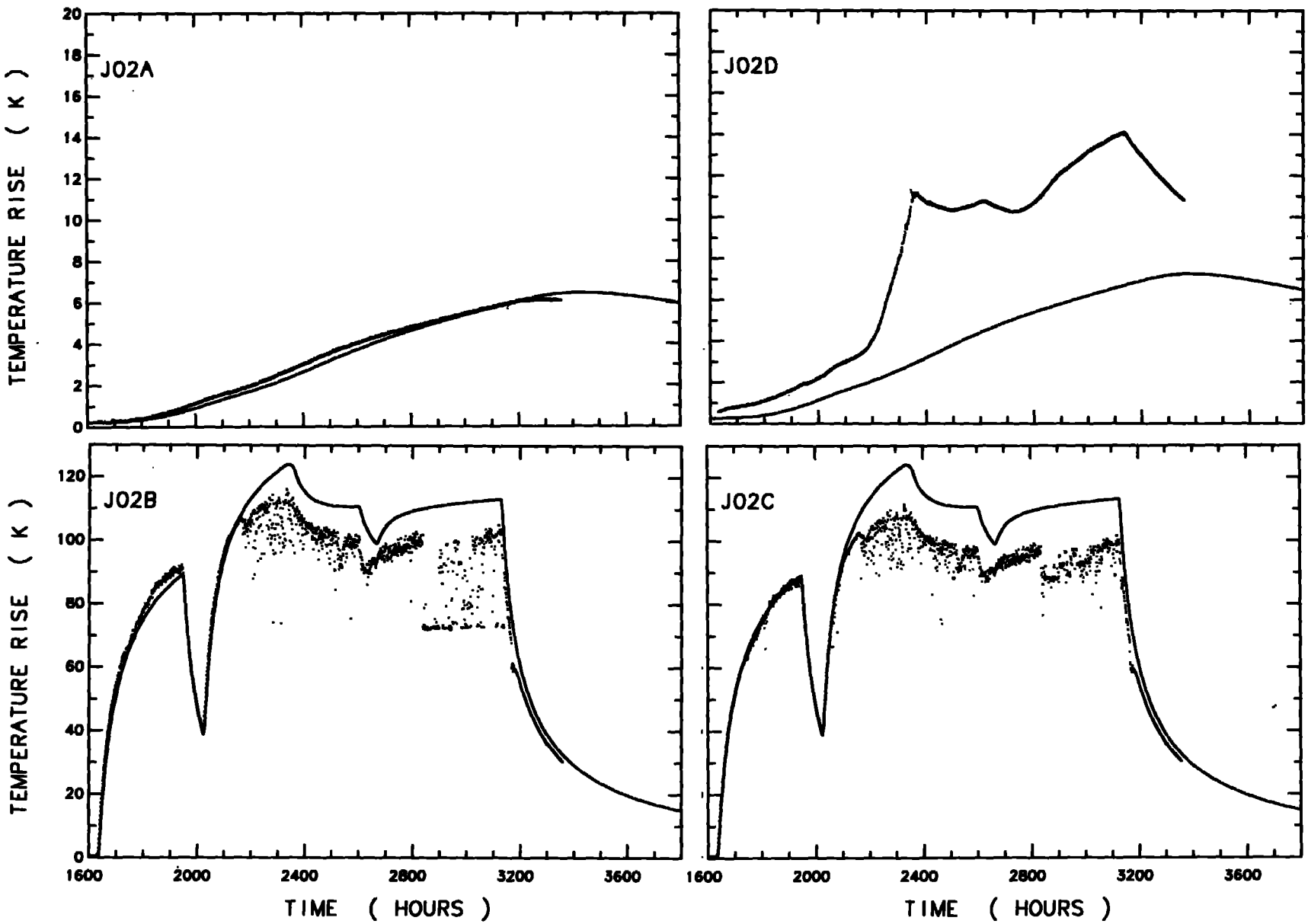

Figure A-8. Calculated and measured temperature histories for test using heater H-2, borehole J-02. Alphabetic codes are A = below heater, B and C = at heater midplane, and D = above heater midplane.

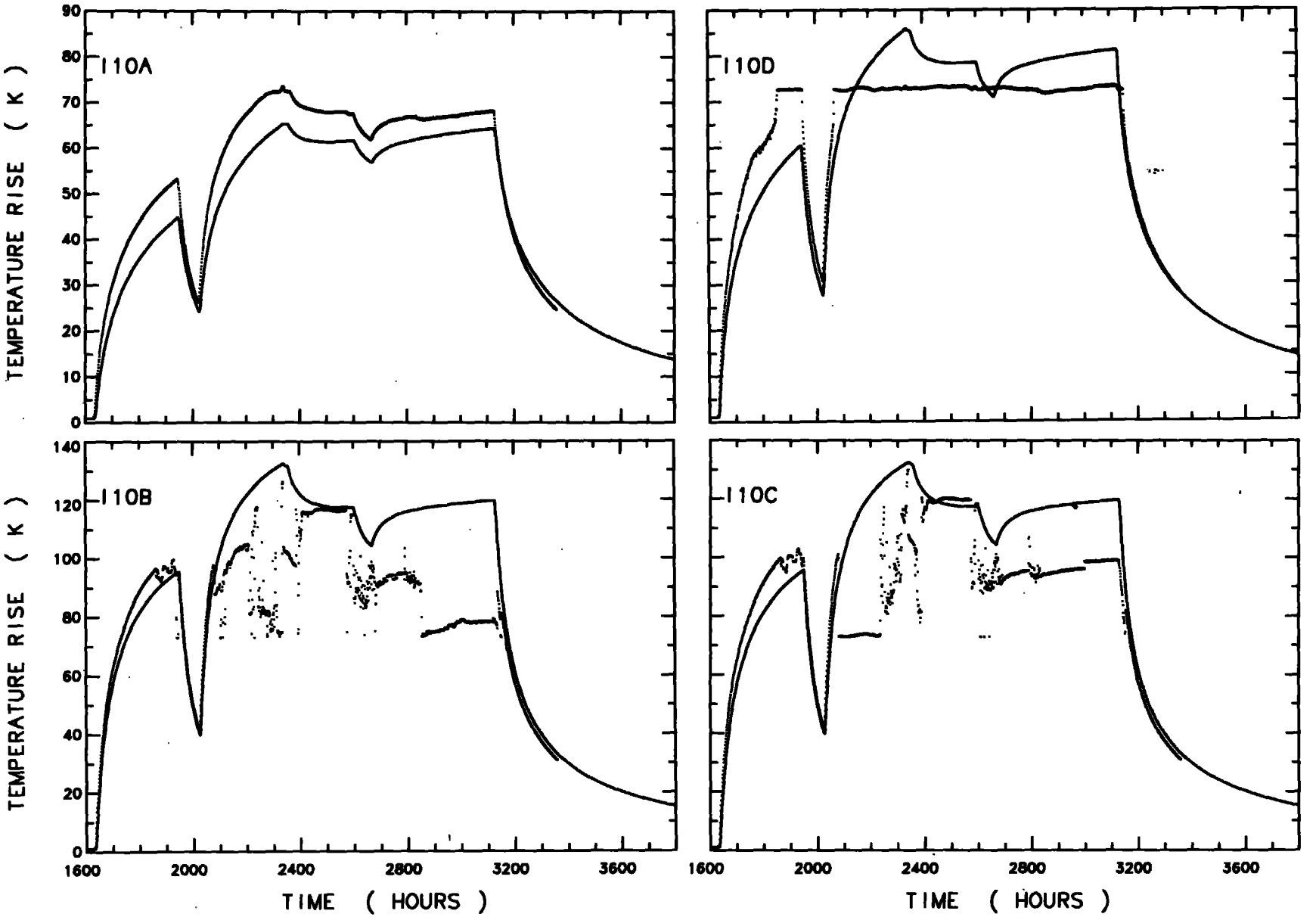

Figure A-9. Calculated and measured temperature histories for test using heater H-2, borehole I-10. Alphabetic codes are A = below heater, B and C = at heater midplane, and D = above heater midplane.

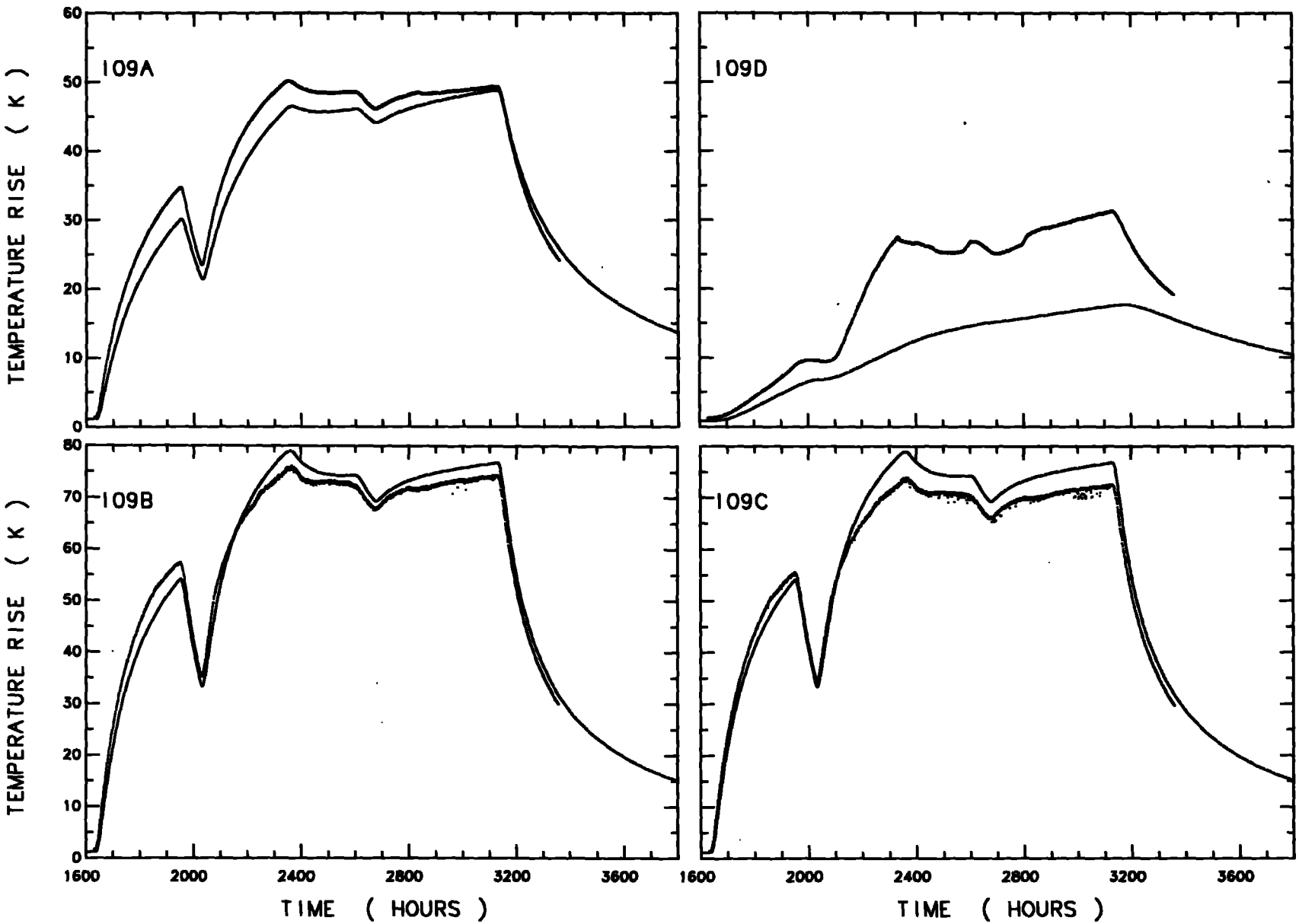

Figure A-10. Calculated and measured temperature histories for test using heater H-2, borehole I-09. Alphabetic codes are A = below heater, B and C = at heater midplane, and D = above heater midplane.

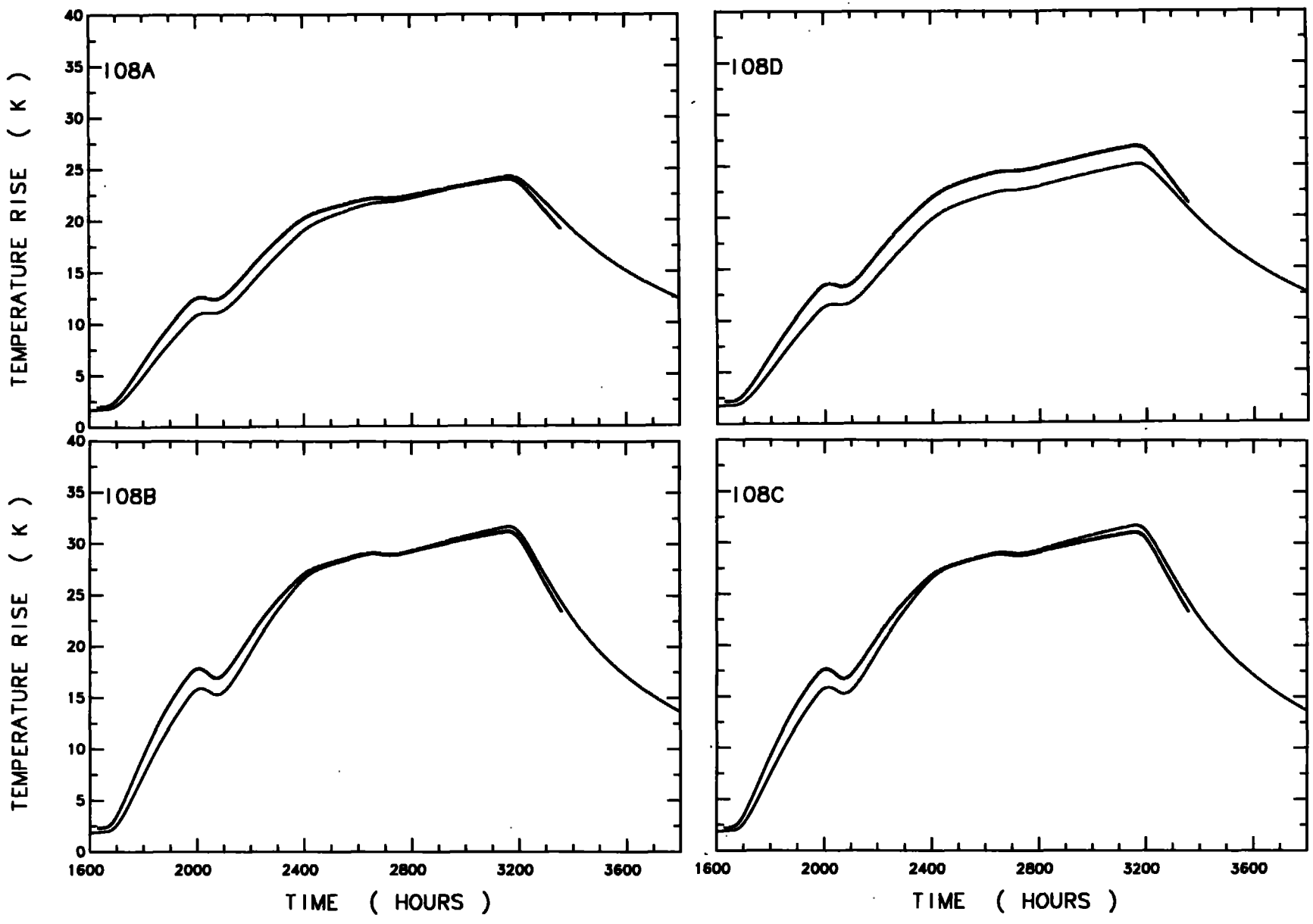

Figure A-11. Calculated and measured temperature histories for test using heater H-2, borehole I-08. Alphabetic codes are A = below heater, B and C = at heater midplane, and D = above heater midplane.

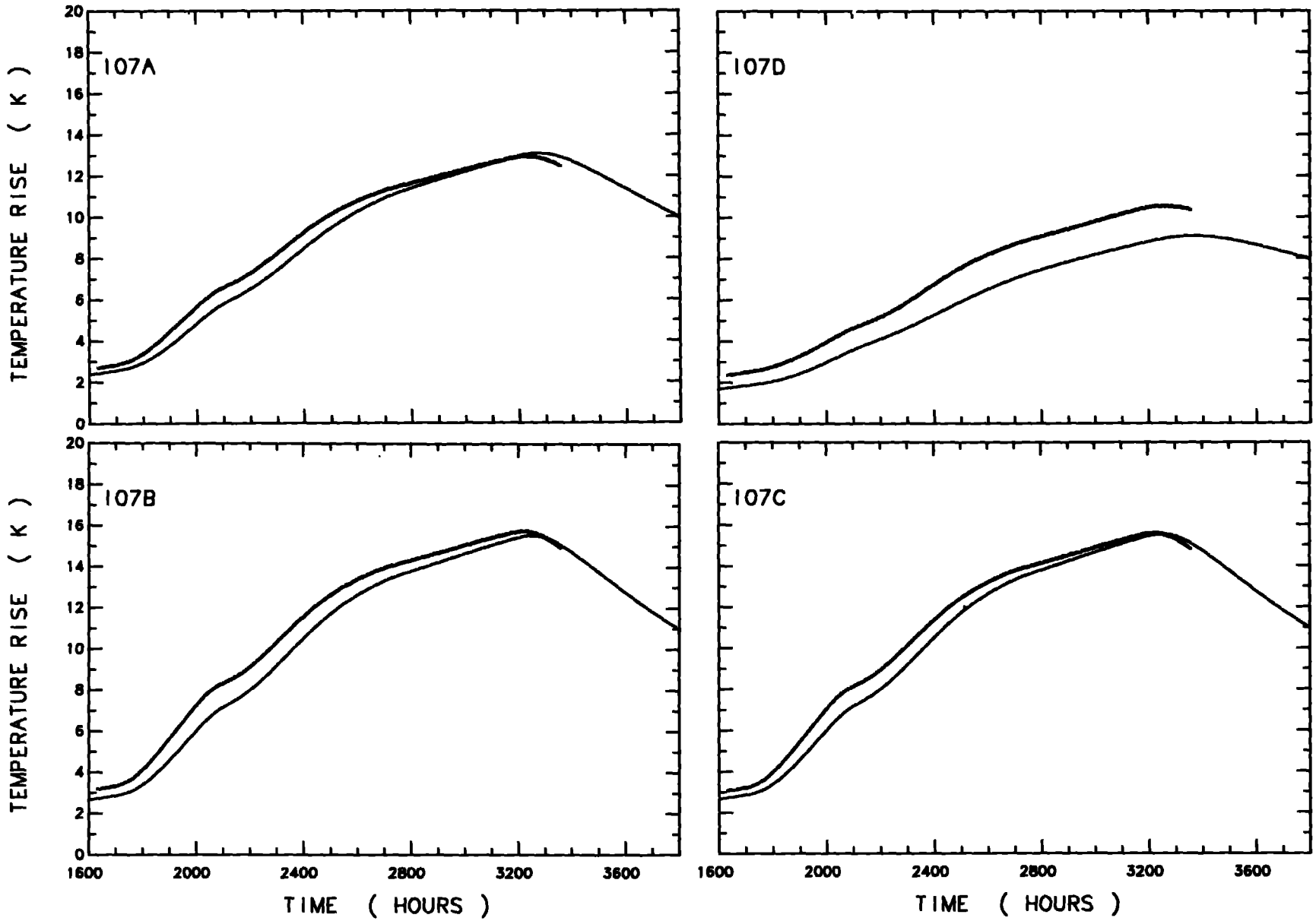

Figure A-12. Calculated and measured temperature histories for test using heater H-2, borehole I-07. Alphabetic codes are A = below heater, B and C = at heater midplane, and D = above heater midplane.

Appendix B
Permeability Test Data and Analysis

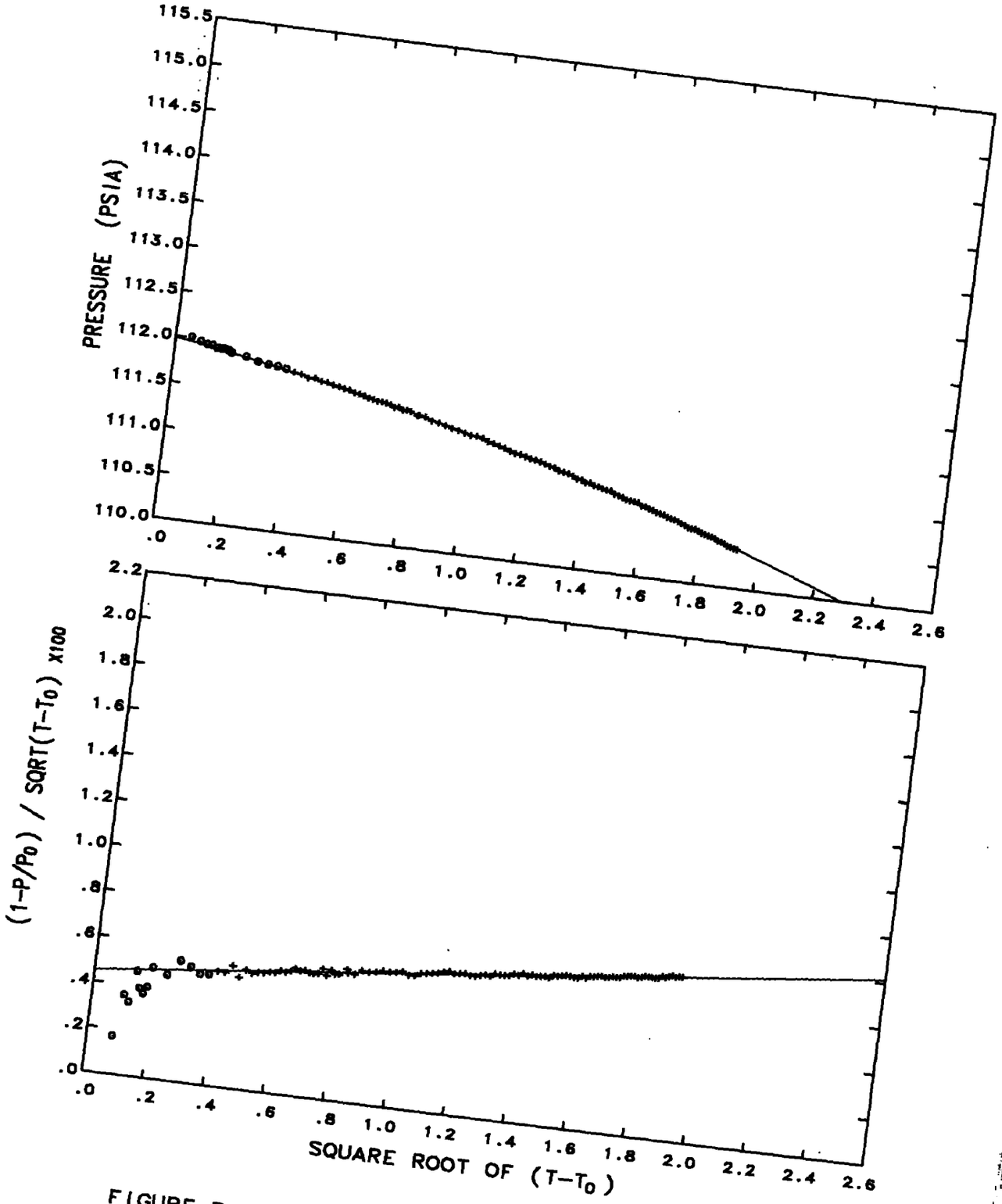

FIGURE B-1. PERMEABILITY TEST M, HOLE J-02,
T_0 = 103.69 DAYS, AVERAGE TEMPERATURE = 32.3 C,
99 OF 113 DATA POINTS USED, RESIDUAL = .007,
PERMEABILITY = .40 ND, POROSITY = .0028 .

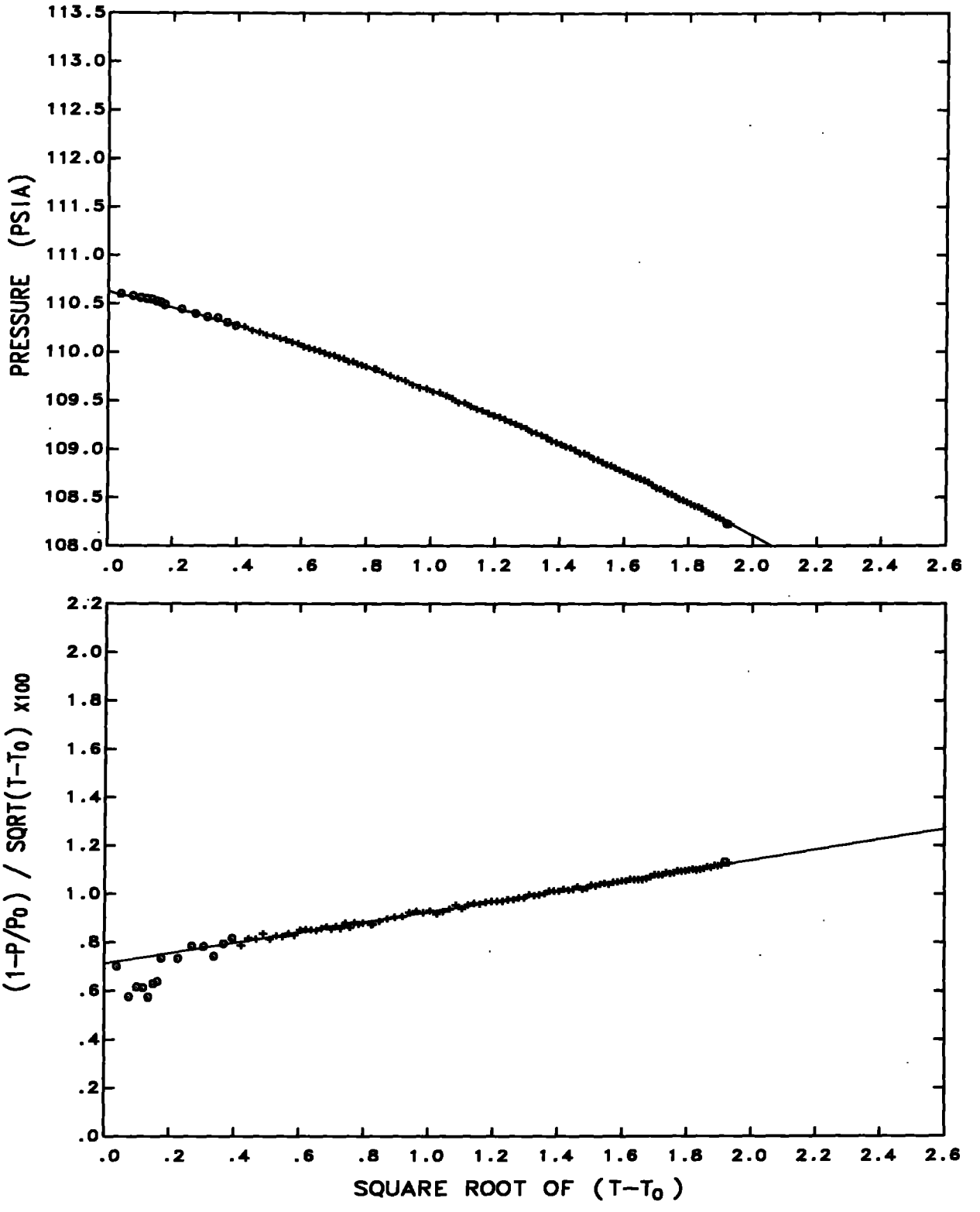

FIGURE B-2. PERMEABILITY TEST M, HOLE I-09, T_0 = 103.70 DAYS, AVERAGE TEMPERATURE = 32.4 C, 97 OF 112 DATA POINTS USED, RESIDUAL = .007, PERMEABILITY = .62 ND, POROSITY = .0047 .

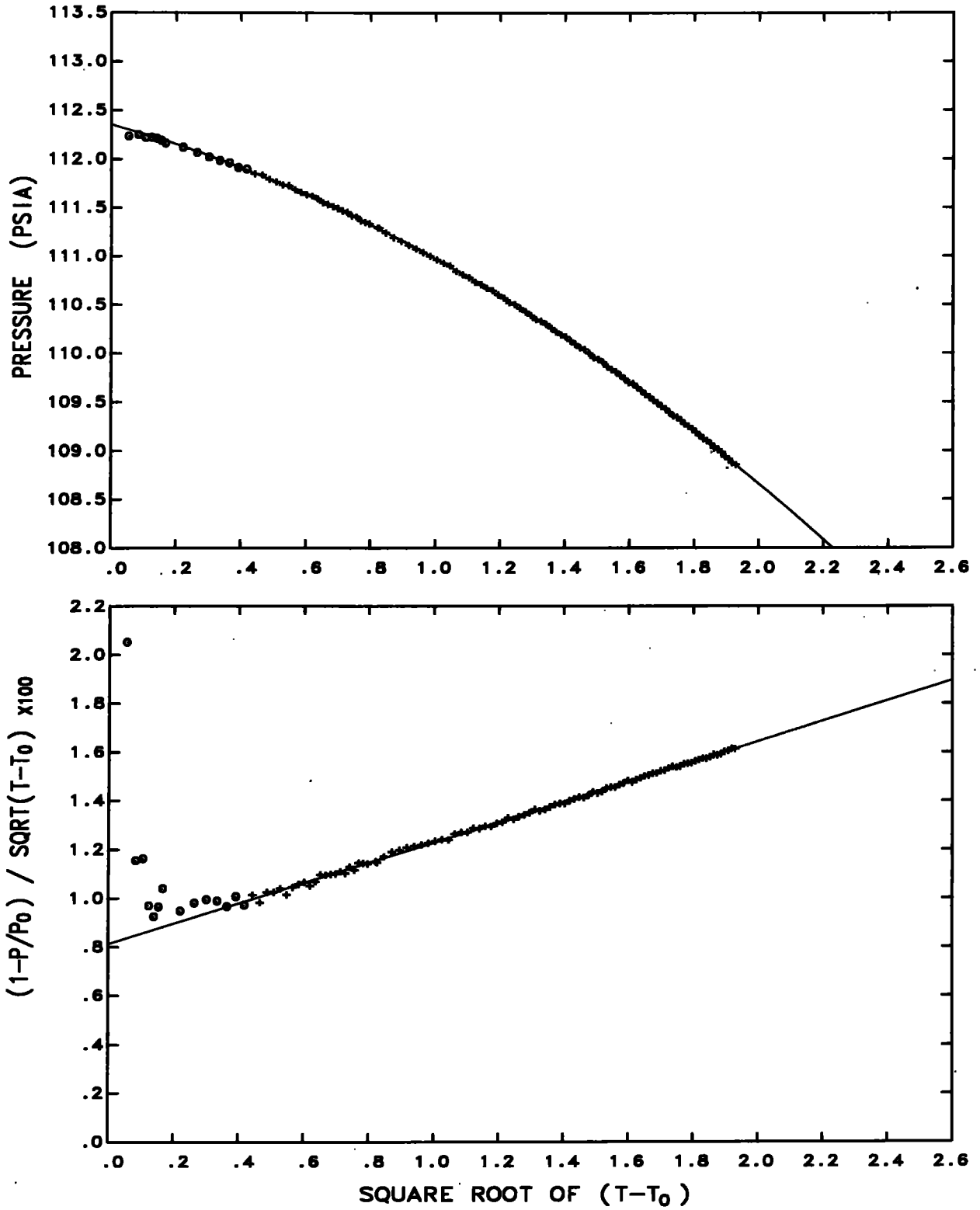

FIGURE B-3. PERMEABILITY TEST M, HOLE I-10, T_0 = 103.70 DAYS, AVERAGE TEMPERATURE = 32.4 C, 97 OF 111 DATA POINTS USED, RESIDUAL = .007, PERMEABILITY = 1.19 ND, POROSITY = .0031 .

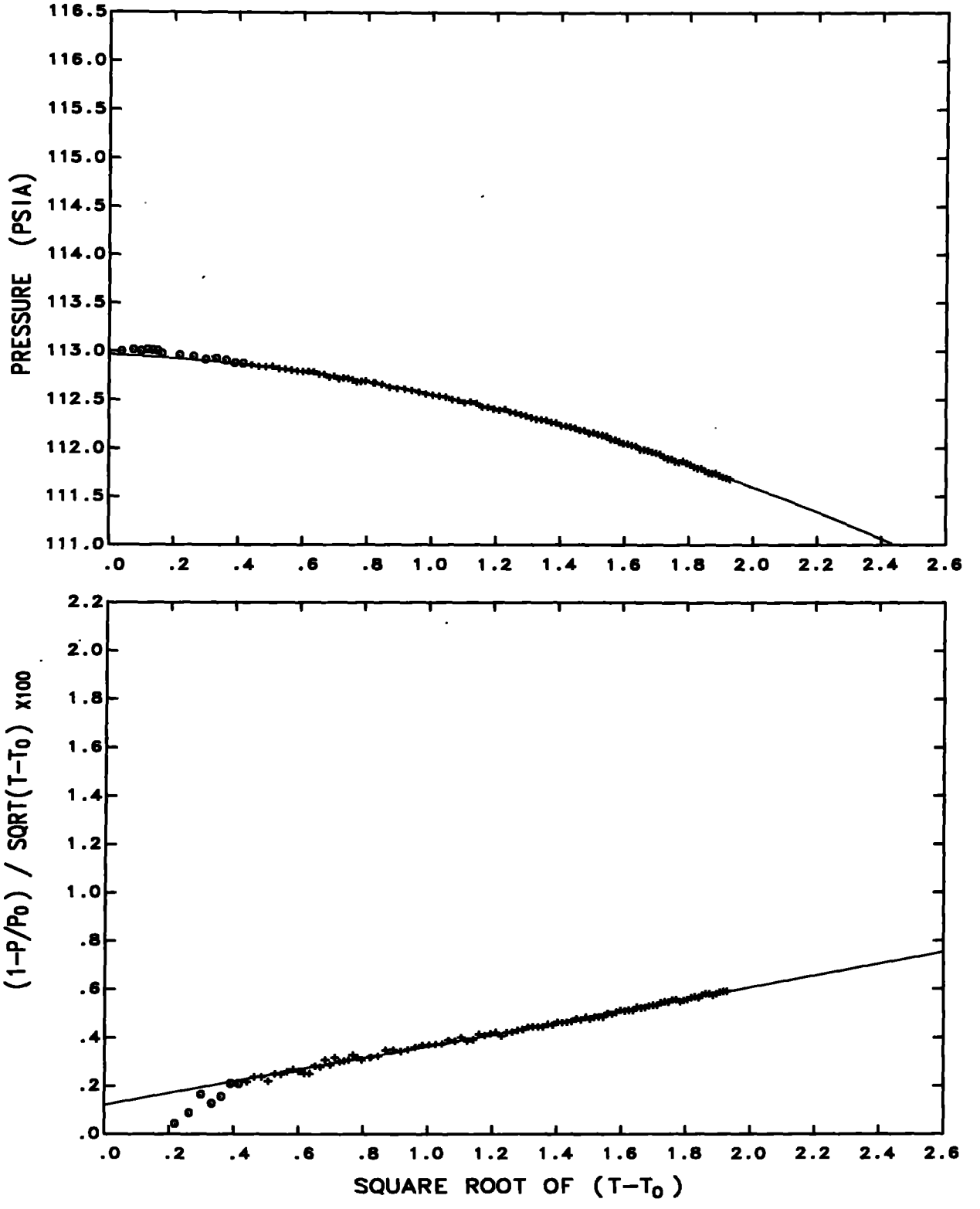

FIGURE B-4. PERMEABILITY TEST M, HOLE I-11, T_0 = 103.70 DAYS, AVERAGE TEMPERATURE = 32.3 C, 97 OF 111 DATA POINTS USED, RESIDUAL = .009, PERMEABILITY = .69 ND, POROSITY = .0001 .

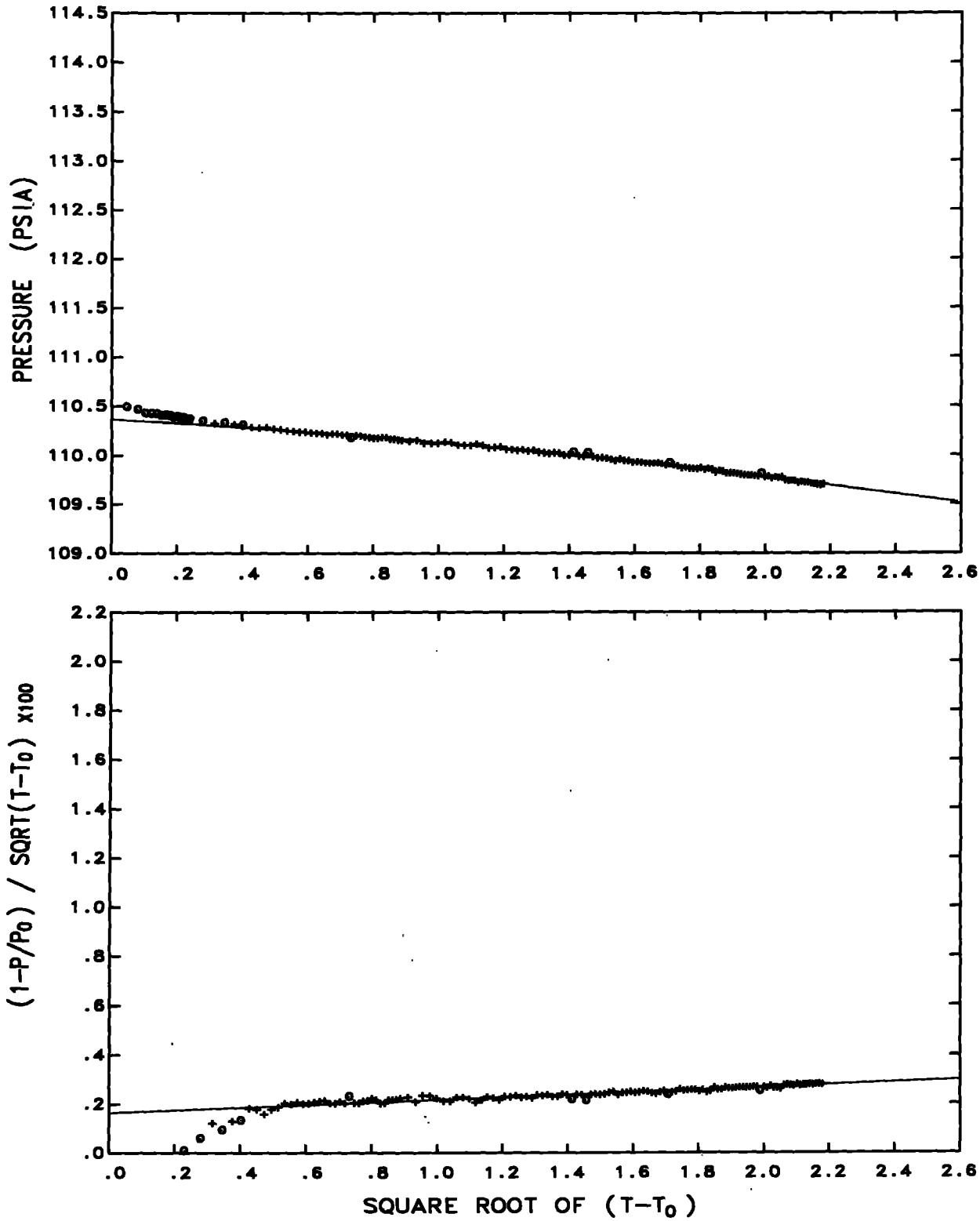

FIGURE B-5. PERMEABILITY TEST N, HOLE J-02, T_0 = 117.59 DAYS, AVERAGE TEMPERATURE = 51.2 C, 122 OF 144 DATA POINTS USED, RESIDUAL = .009, PERMEABILITY = .15 ND, POROSITY = .0010 .

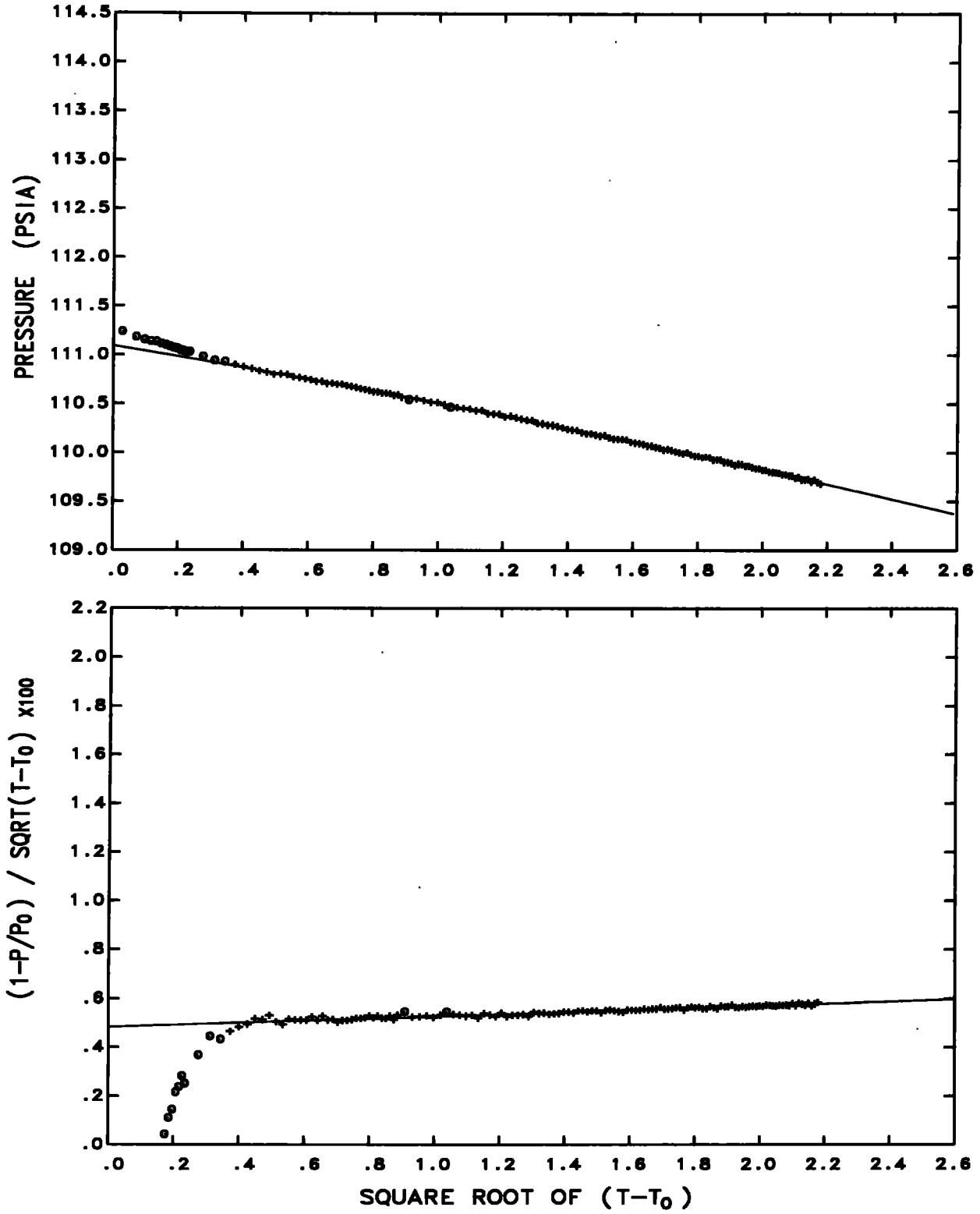

FIGURE B-6. PERMEABILITY TEST N, HOLE I-09, T_0 = 117.59 DAYS, AVERAGE TEMPERATURE = 43.6 C, 125 OF 144 DATA POINTS USED, RESIDUAL = .007, PERMEABILITY = .13 ND, POROSITY = .0103 .

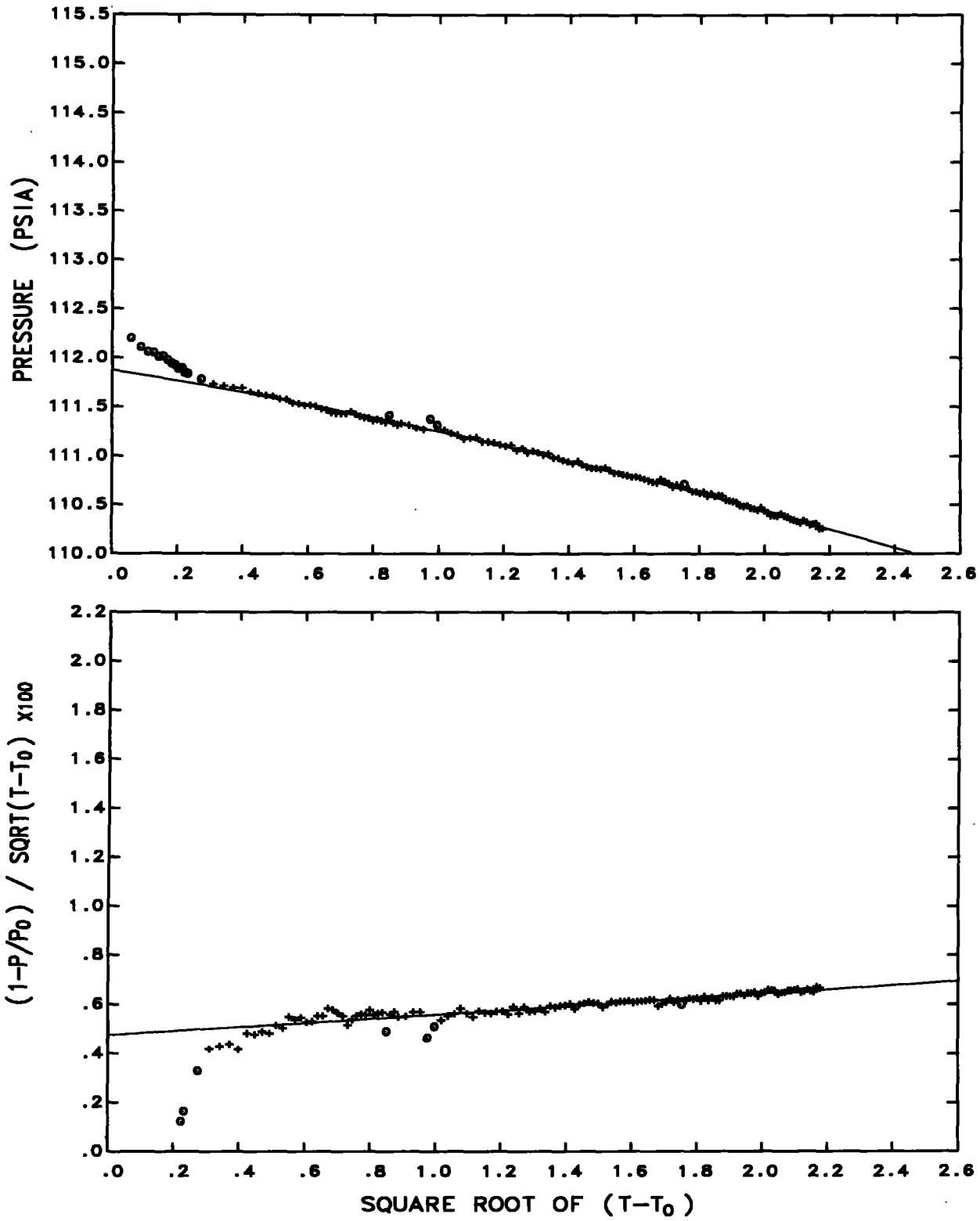

FIGURE B-7. PERMEABILITY TEST N, HOLE I-10, T_0 = 117.59 DAYS, AVERAGE TEMPERATURE = 53.4 C, 125 OF 143 DATA POINTS USED, RESIDUAL = .017, PERMEABILITY = .24 ND, POROSITY = .0053 .

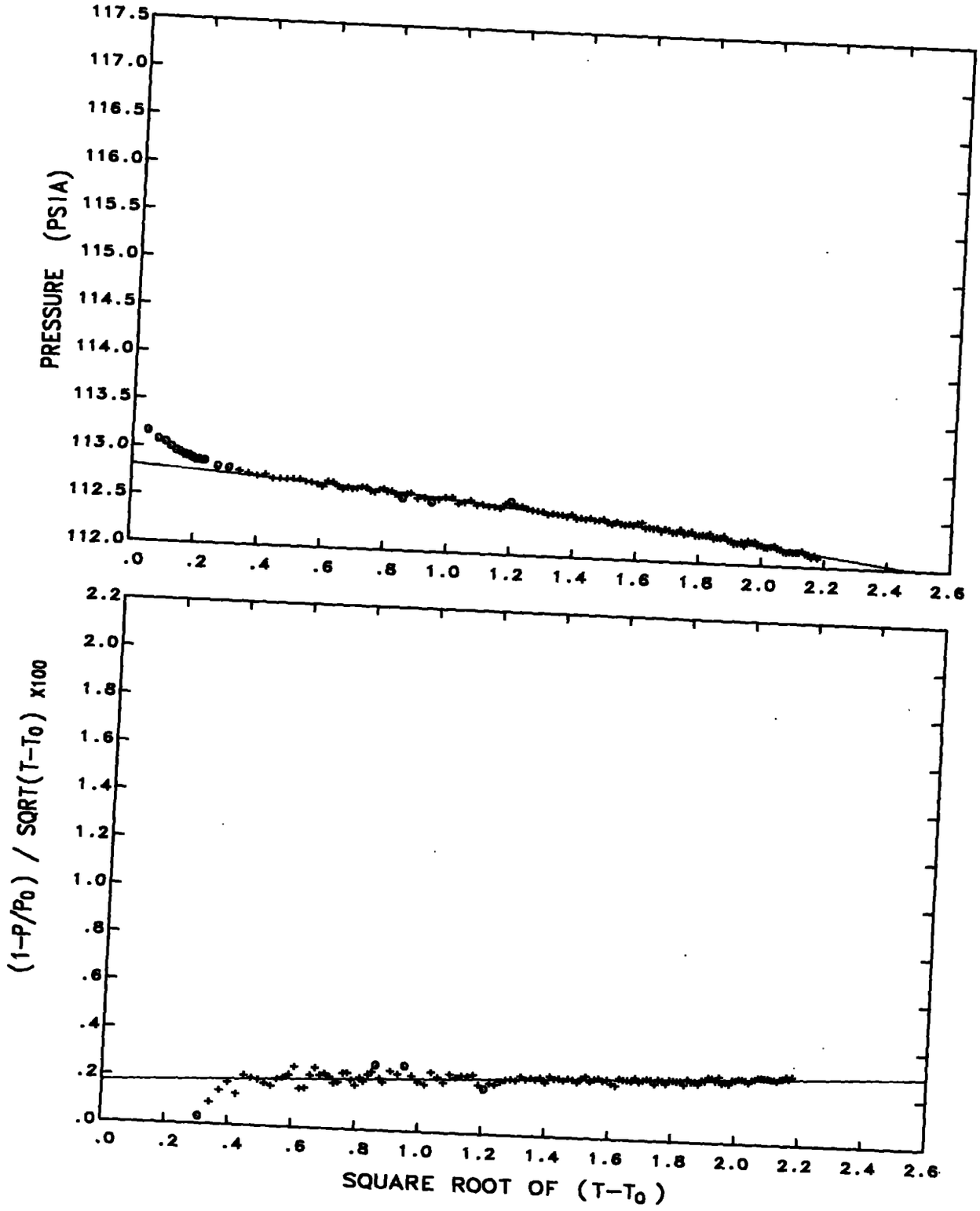

FIGURE B-8. PERMEABILITY TEST N, HOLE I-11, T_0 = 117.59 DAYS, AVERAGE TEMPERATURE = 51.3 C, 125 OF 143 DATA POINTS USED, RESIDUAL = .018, PERMEABILITY = .13 ND, POROSITY = .0012 .

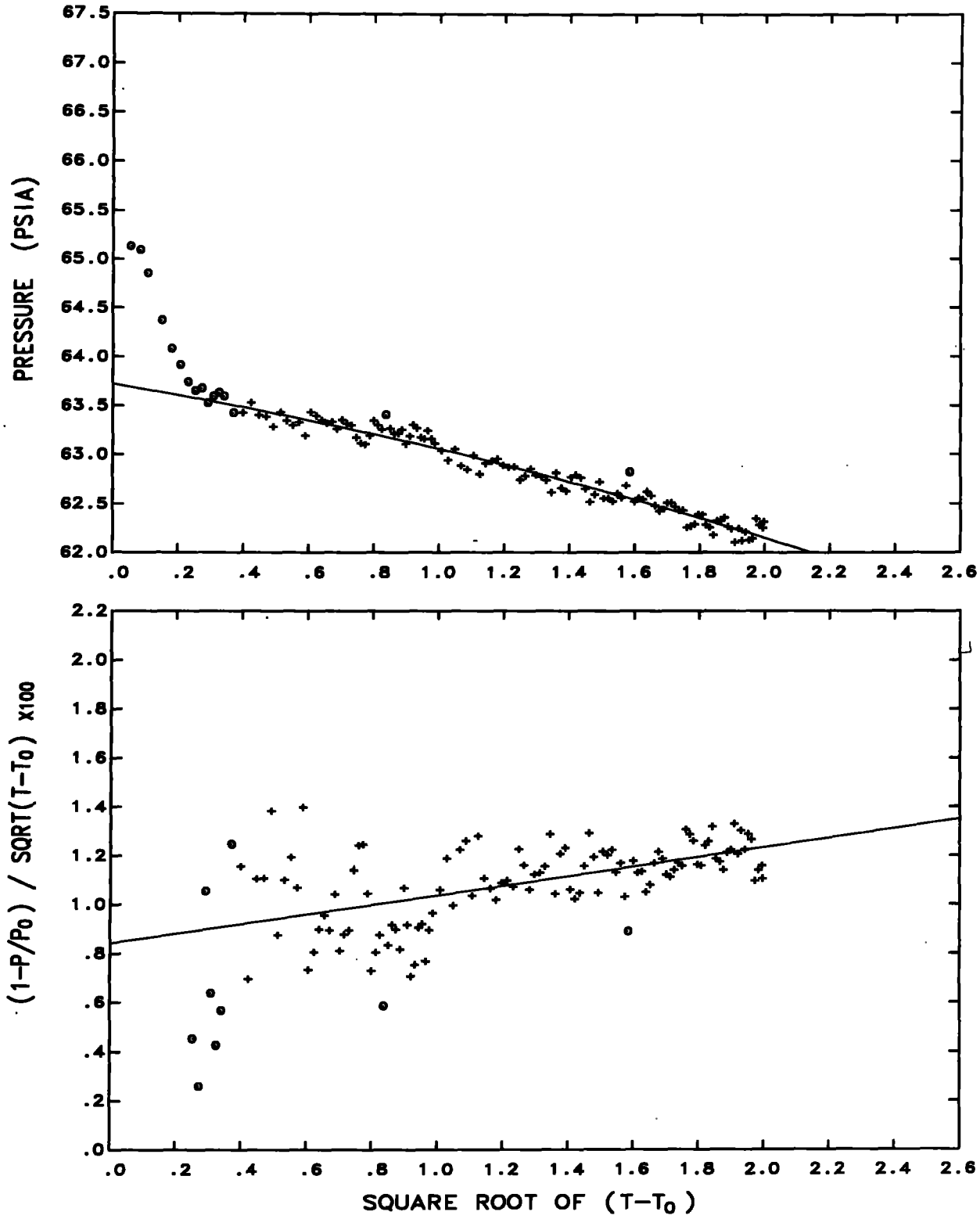

FIGURE B-9. PERMEABILITY TEST O, HOLE H-02, T_0 = 138.36 DAYS, AVERAGE TEMPERATURE = 419.3 C, 111 OF 127 DATA POINTS USED, RESIDUAL = .082, PERMEABILITY = 1.09 ND, POROSITY = .0071 .

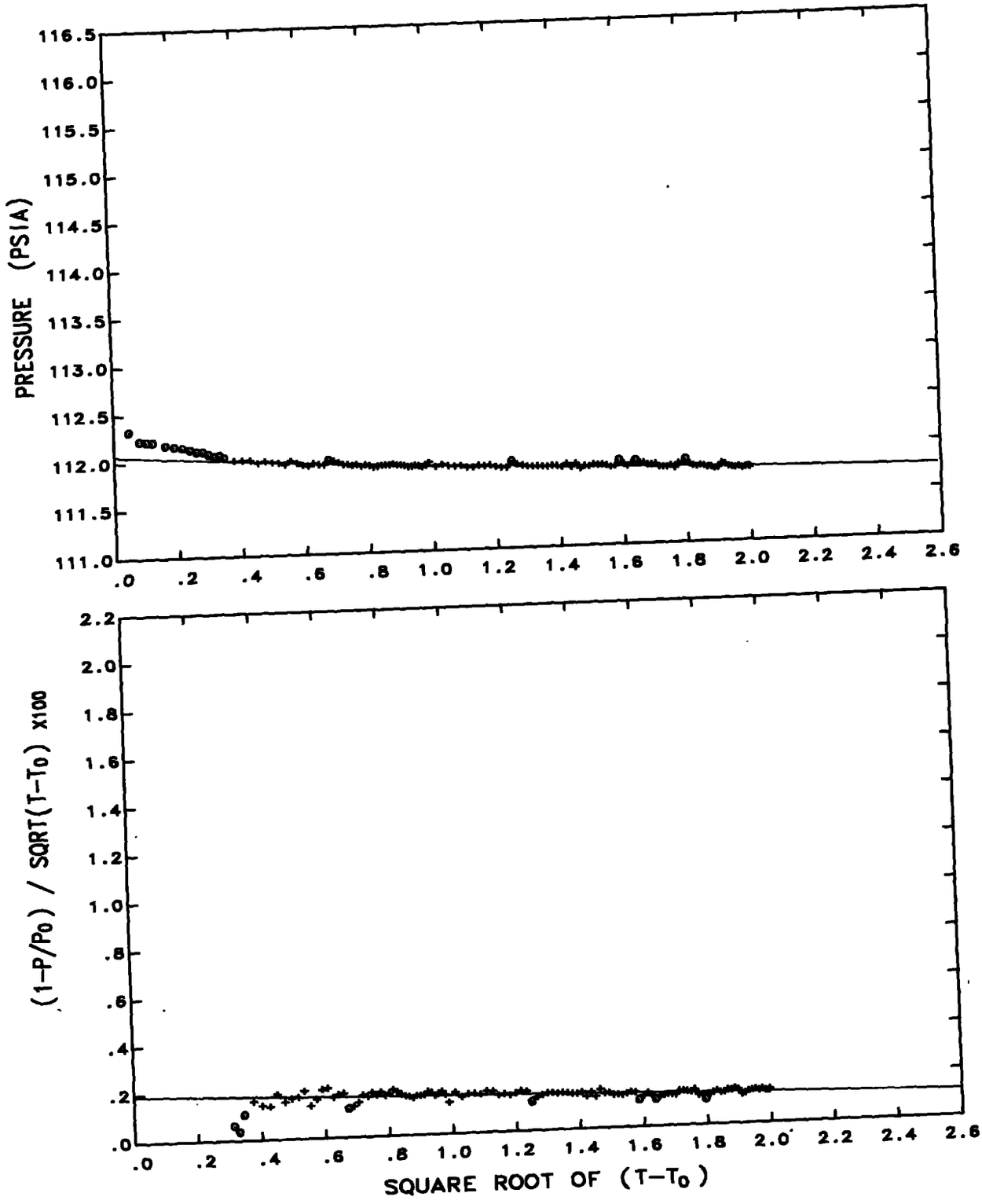

FIGURE B-10. PERMEABILITY TEST O, HOLE J-02, T_0 = 138.36 DAYS, AVERAGE TEMPERATURE = 74.3 C, 109 OF 128 DATA POINTS USED, RESIDUAL = .015, PERMEABILITY = -.09 ND, POROSITY = -.0024

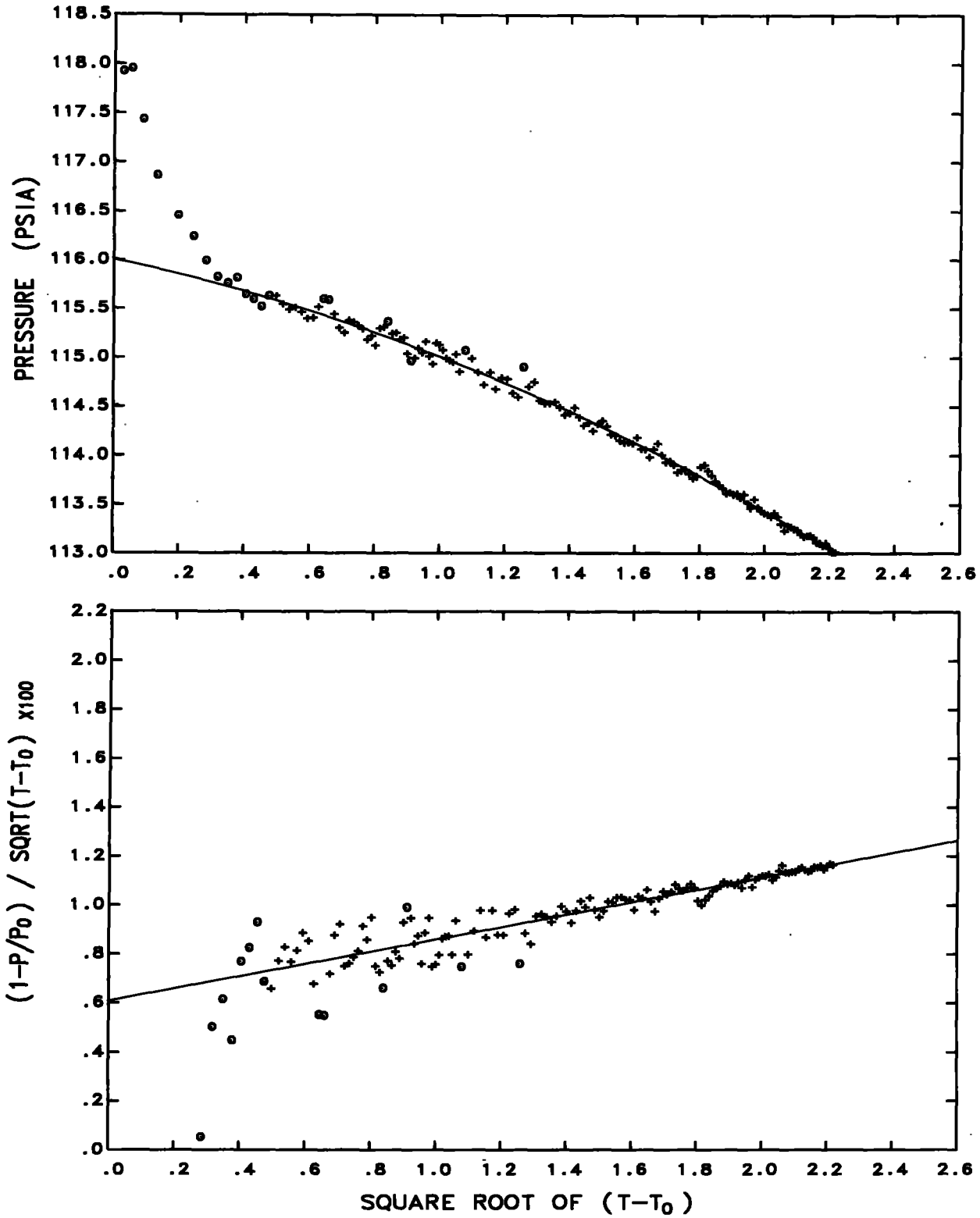

FIGURE B-11. PERMEABILITY TEST P, HOLE I-09, T_0 = 151.42 DAYS, AVERAGE TEMPERATURE = 70.9 C, 128 OF 148 DATA POINTS USED, RESIDUAL = .060, PERMEABILITY = .70 ND, POROSITY = .0029 .

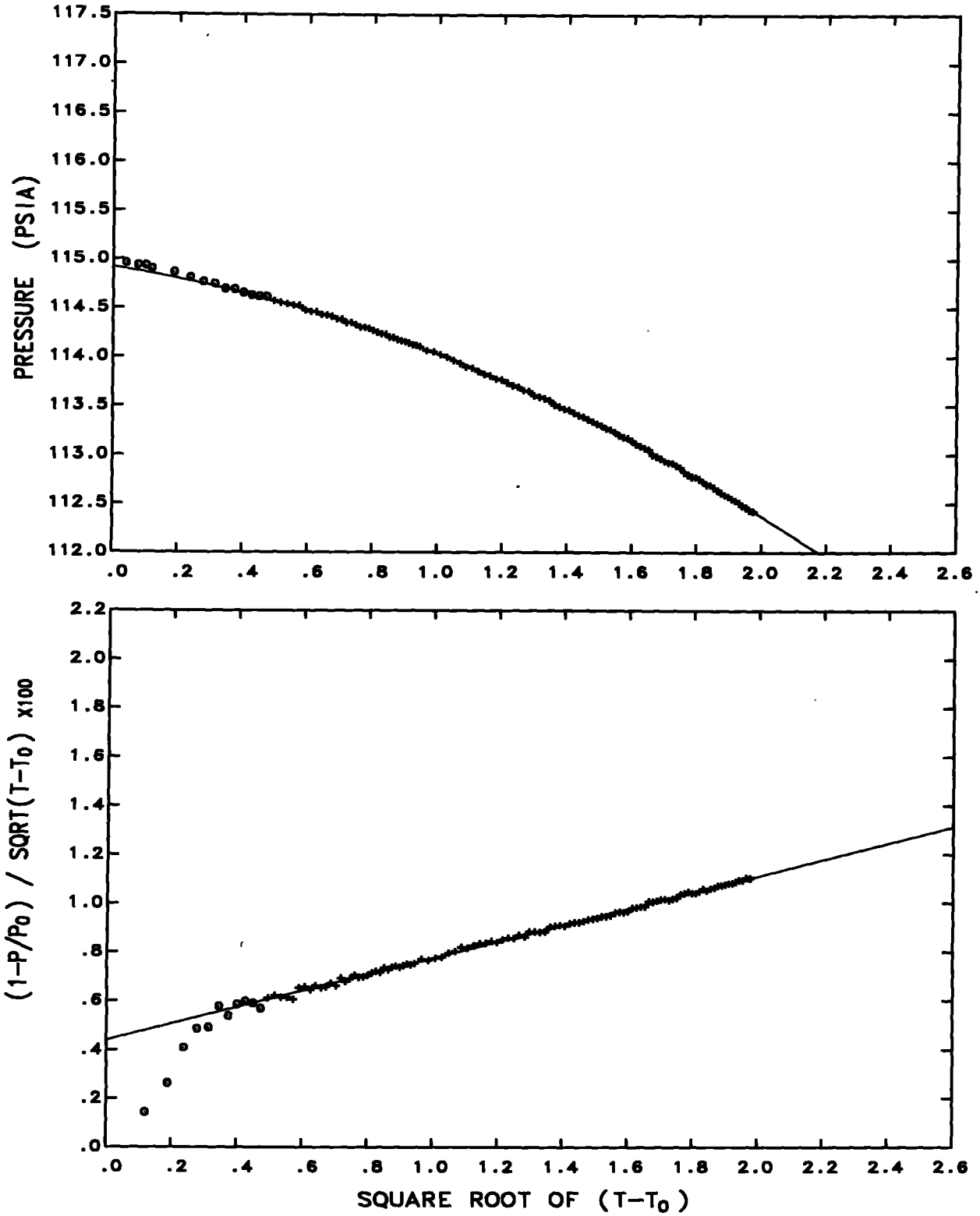

FIGURE B-12. PERMEABILITY TEST Q, HOLE I-09, T_0 = 159.45 DAYS, AVERAGE TEMPERATURE = 46.8 C, 105 OF 119 DATA POINTS USED, RESIDUAL = .009, PERMEABILITY = .93 ND, POROSITY = .0011 .

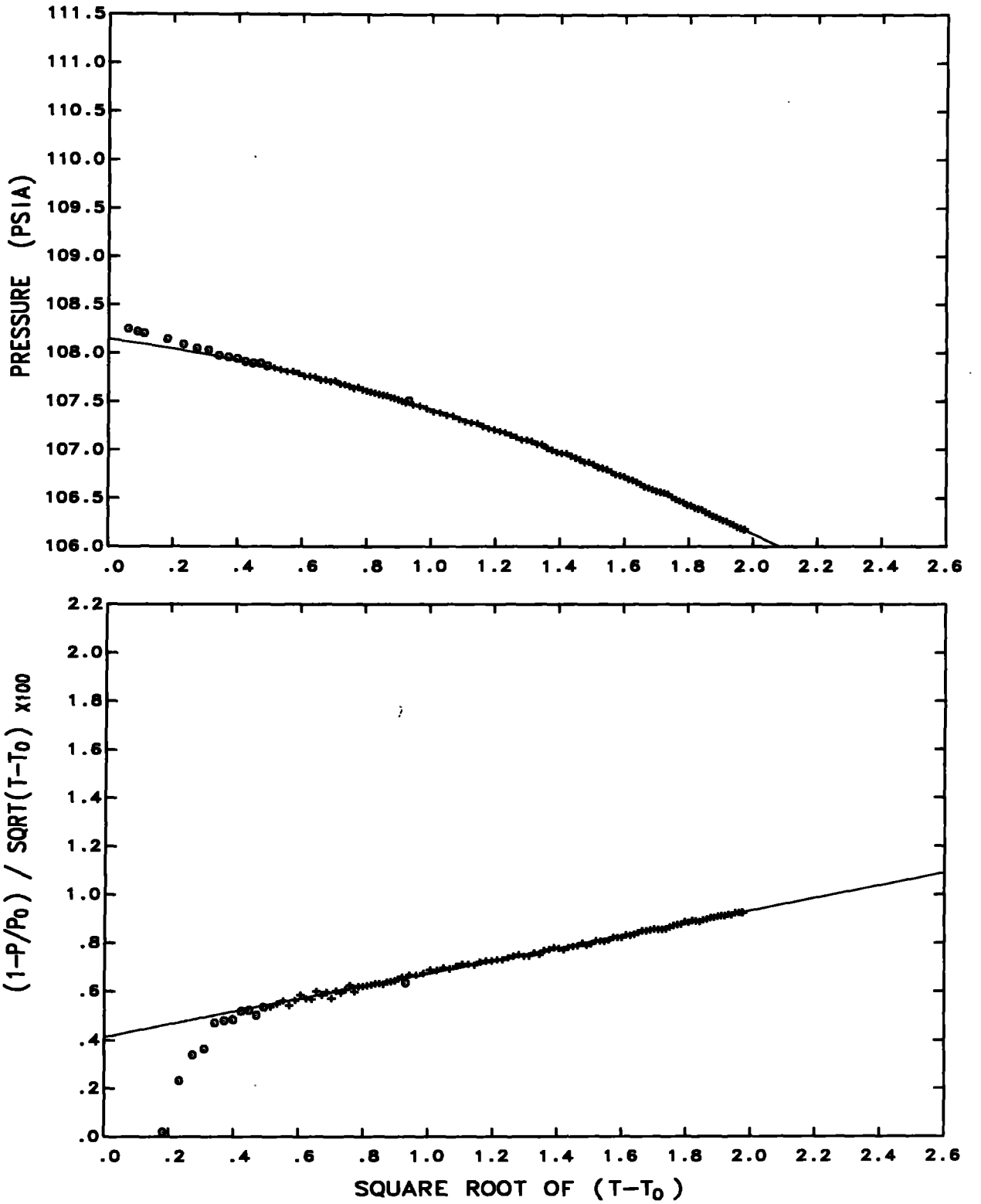

FIGURE B-13. PERMEABILITY TEST Q, HOLE I-10, T_0 = 159.45 DAYS, AVERAGE TEMPERATURE = 47.7 C, 103 OF 118 DATA POINTS USED, RESIDUAL = .008, PERMEABILITY = .78 ND, POROSITY = .0013 .

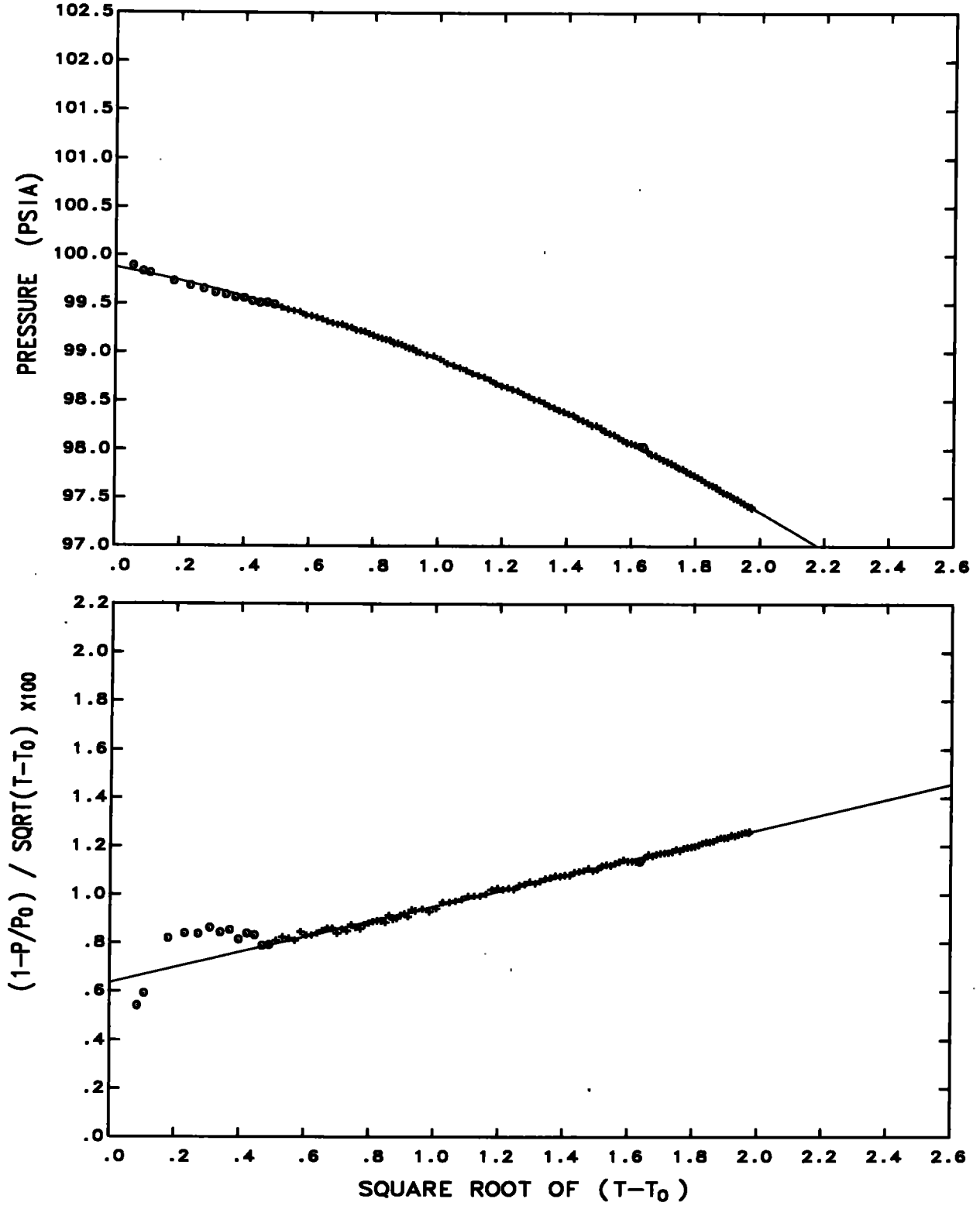

FIGURE B-14. PERMEABILITY TEST Q, HOLE I-11, T_0 = 159.45 DAYS, AVERAGE TEMPERATURE = 47.5 C, 103 OF 118 DATA POINTS USED, RESIDUAL = .008, PERMEABILITY = 1.03 ND, POROSITY = .0025 .

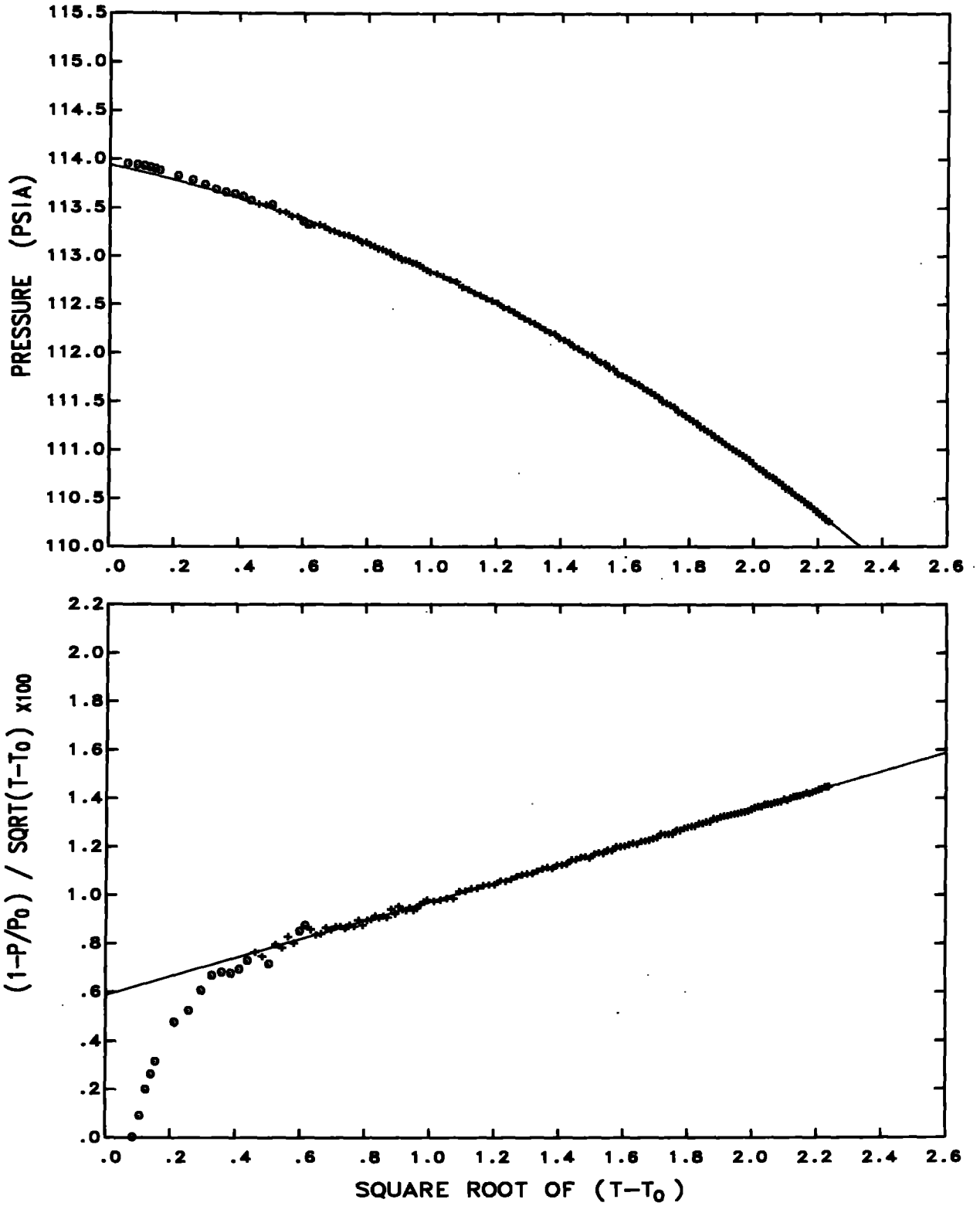

FIGURE B-15. PERMEABILITY TEST R, HOLE I-09, T_0 = 172.35 DAYS, AVERAGE TEMPERATURE = 36.4 C, 132 OF 149 DATA POINTS USED, RESIDUAL = .008, PERMEABILITY = 1.08 ND, POROSITY = .0018 .

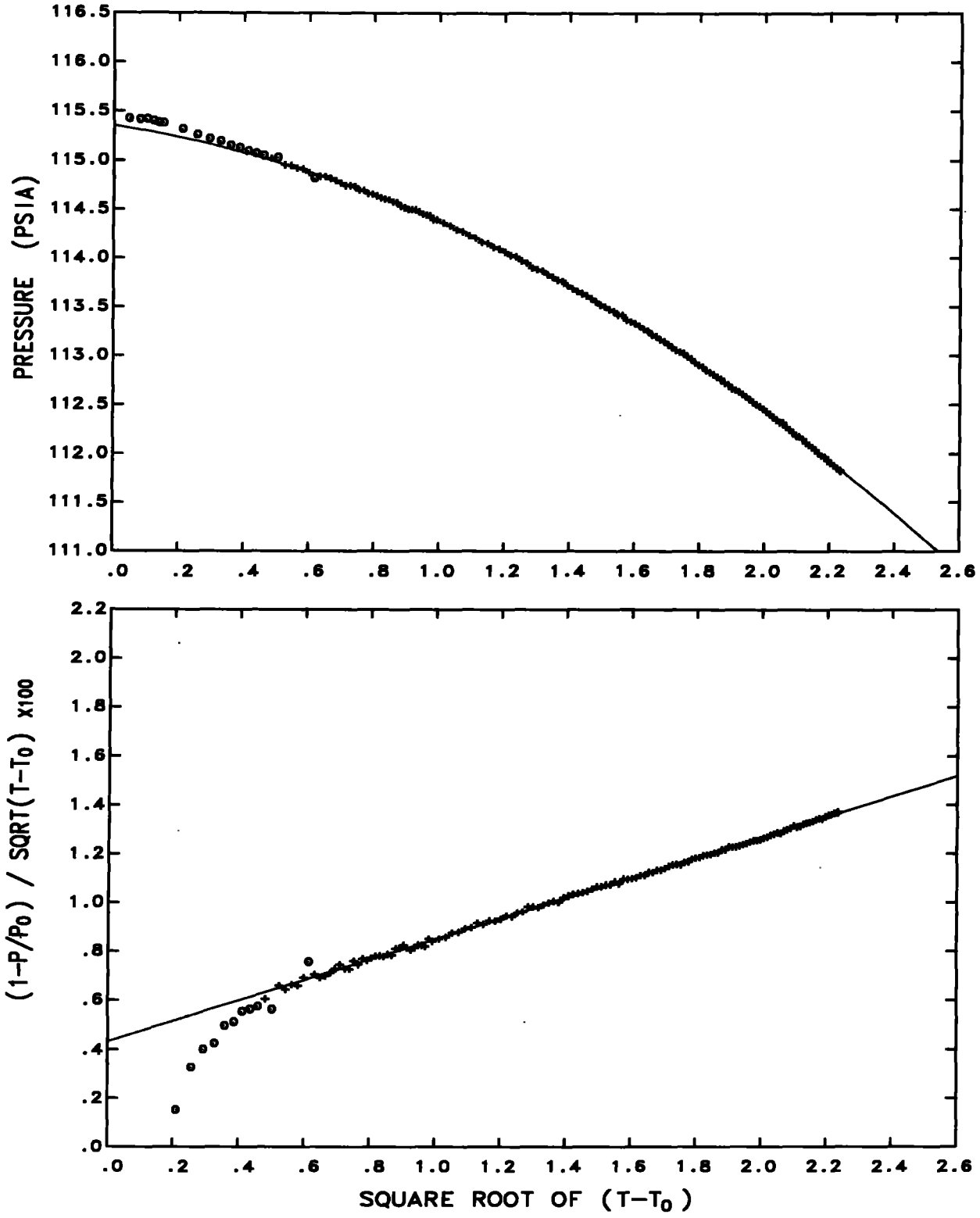

FIGURE B-16. PERMEABILITY TEST R, HOLE I-10, T_0 = 172.35 DAYS, AVERAGE TEMPERATURE = 36.6 C, 132 OF 149 DATA POINTS USED, RESIDUAL = .009, PERMEABILITY = 1.16 ND, POROSITY = .0009 .

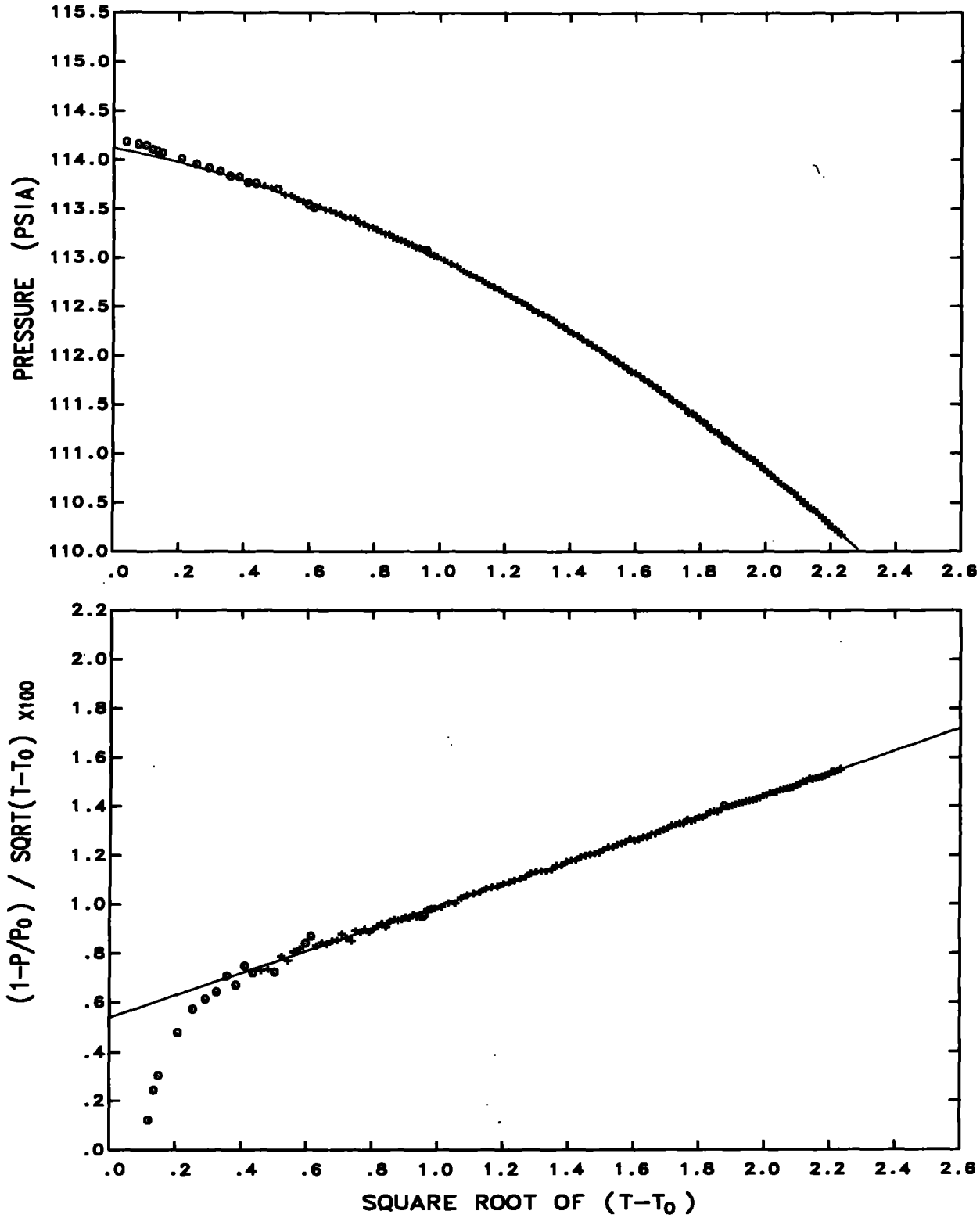

FIGURE B-17. PERMEABILITY TEST R, HOLE I-11, T_0 = 172.35 DAYS, AVERAGE TEMPERATURE = 36.5 C, 130 OF 149 DATA POINTS USED, RESIDUAL = .007, PERMEABILITY = 1.27 ND, POROSITY = .0013 .

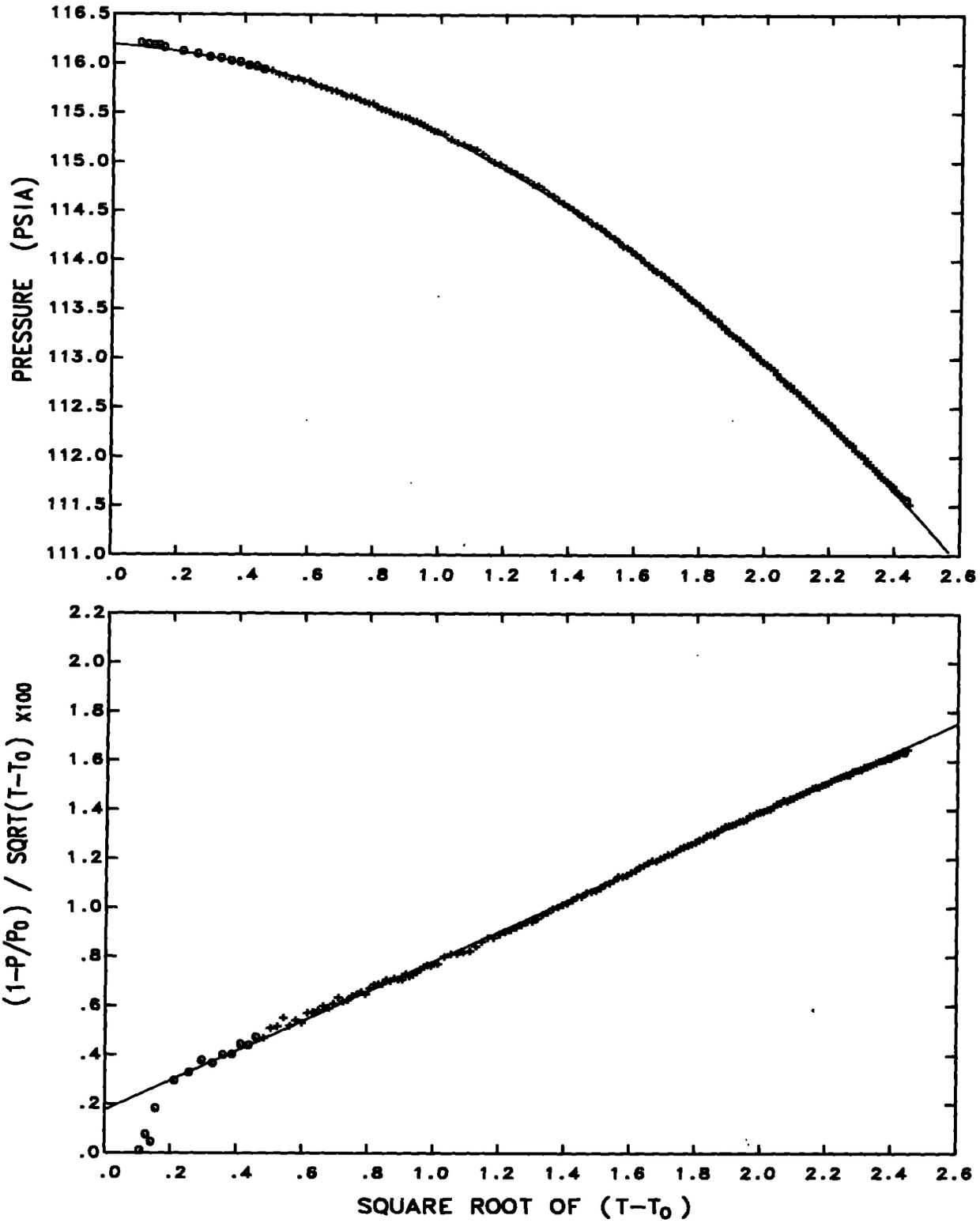

FIGURE B-18. PERMEABILITY TEST S, HOLE P-01, T_0 = 180.35 DAYS, AVERAGE TEMPERATURE = 28.2 C, 156 OF 171 DATA POINTS USED, RESIDUAL = .015, PERMEABILITY = 1.67 ND, POROSITY = .0001 .

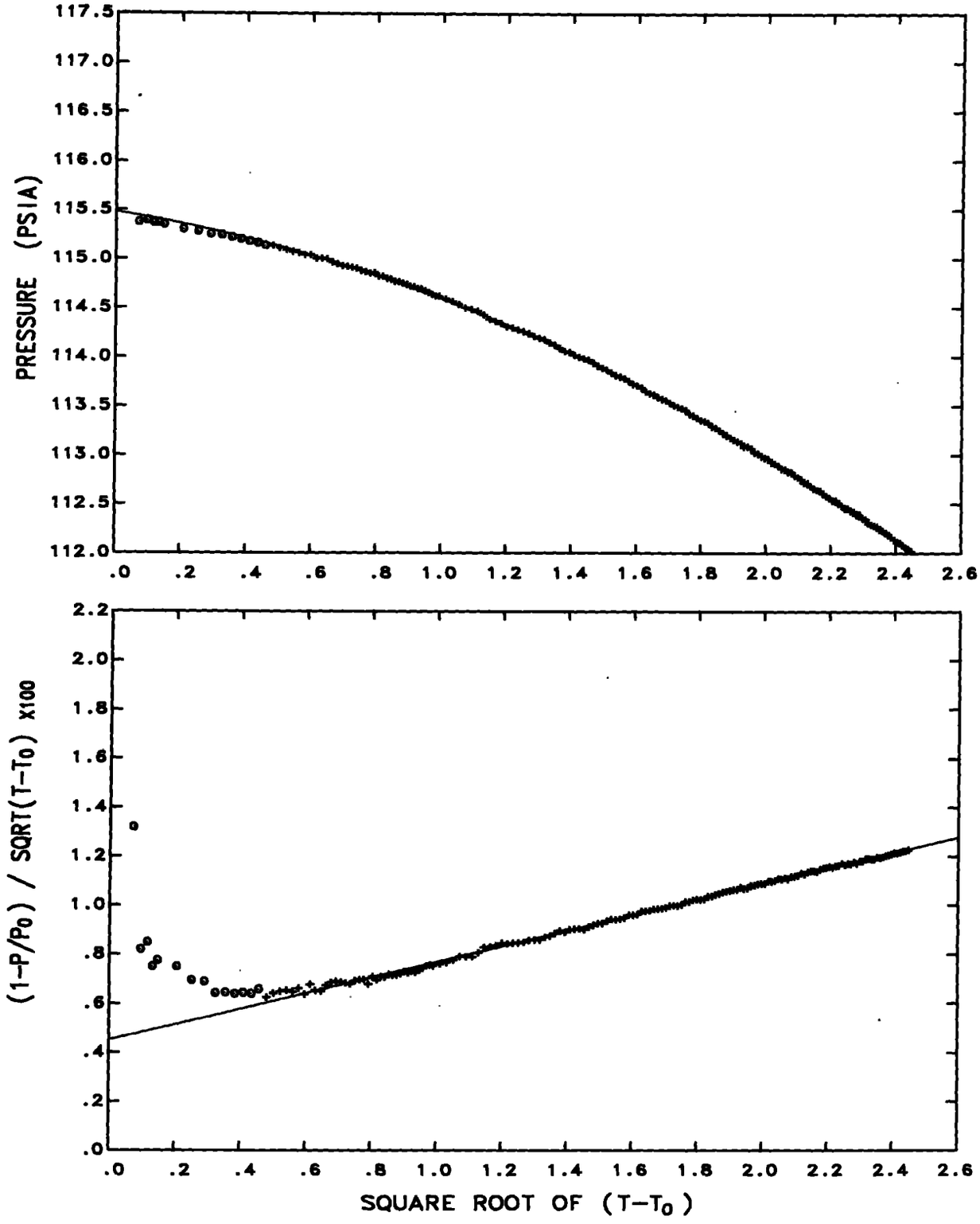

FIGURE B-19. PERMEABILITY TEST S, HOLE I-06, T_0 = 180.35 DAYS, AVERAGE TEMPERATURE = 28.7 C, 157 OF 171 DATA POINTS USED, RESIDUAL = .010, PERMEABILITY = .88 ND, POROSITY = .0013 .

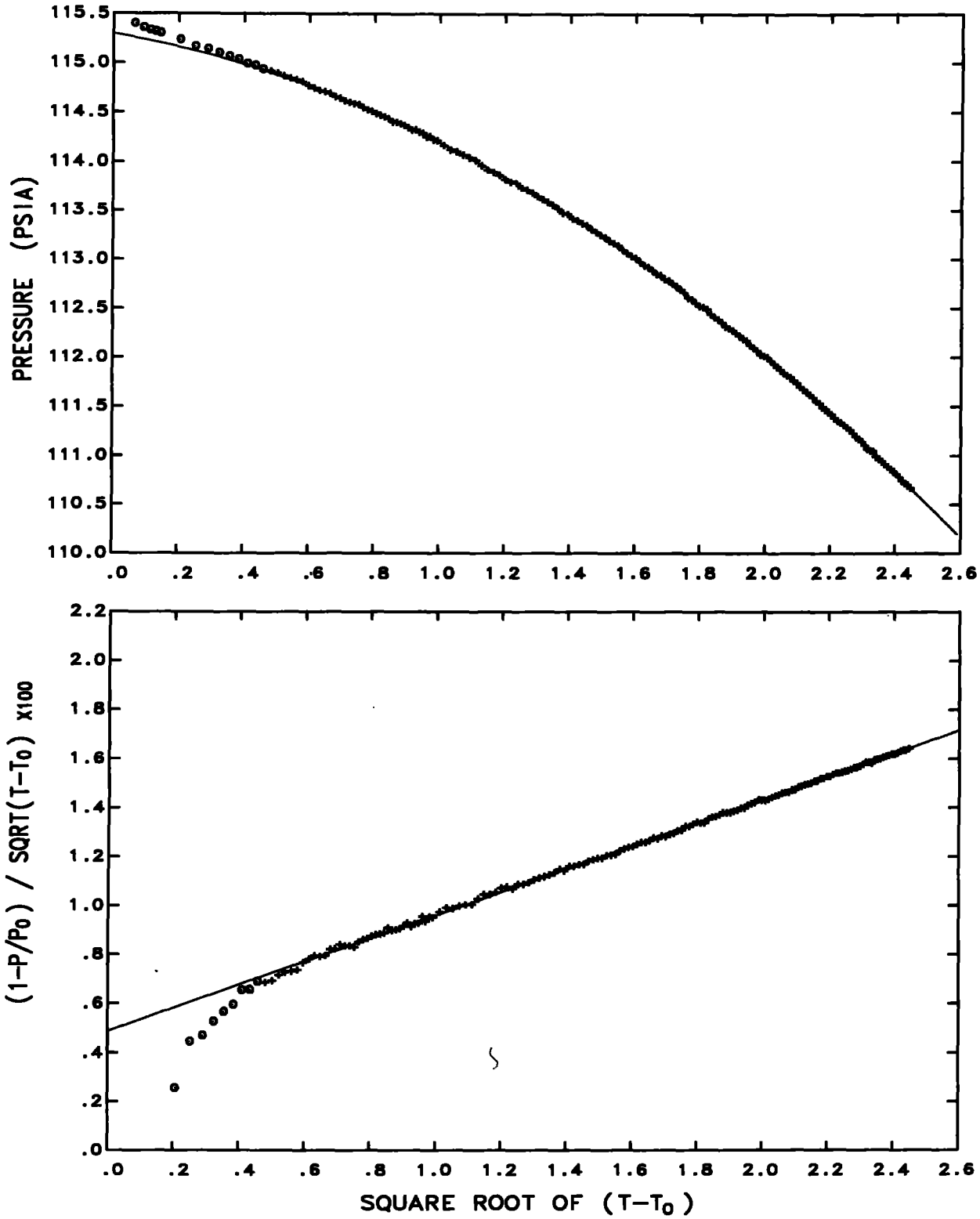

FIGURE B-20. PERMEABILITY TEST S, HOLE I-11, T_0 = 180.35 DAYS, AVERAGE TEMPERATURE = 33.7 C, 157 OF 171 DATA POINTS USED, RESIDUAL = .009, PERMEABILITY = 1.31 ND, POROSITY = .0010 .